FE-2030-5

CHARACTERISTICS OF AMERICAN COALS IN RELATION TO THEIR CONVERSION INTO CLEAN ENERGY FUELS

Quarterly Technical Progress Report, July—September, 1976

December 1976

Work Performed Under Contract No. EX-76-C-01-2030

Coal Research Section
Pennsylvania State University
University Park, Pennsylvania

ENERGY RESEARCH AND DEVELOPMENT ADMINISTRATION

DISCLAIMER

NOTICE

This report has been reproduced directly from the best available copy.

Available from the National Technical Information Service, U. S. Department of Commerce, Springfield, Virginia 22161

Price: Paper Copy $5.00 (domestic)
$7.50 (foreign)
Microfiche $3.00 (domestic)
$4.50 (foreign)

FE-2030-5
Distribution Category UC-90a, b, c, d & e

THE CHARACTERISTICS OF AMERICAN COALS IN RELATION TO THEIR CONVERSION INTO CLEAN ENERGY FUELS

Quarterly Technical Progress Report

July - September 1976

by

W. Spackman, A. Davis, P.L. Walker, H.L. Lovell,
R.H. Essenhigh, F.J. Vastola and P.H. Given

COAL RESEARCH SECTION
THE PENNSYLVANIA STATE UNIVERSITY
UNIVERSITY PARK, PENNSYLVANIA 16802

THIS PAGE

WAS INTENTIONALLY

LEFT BLANK

ABSTRACT

Under Facet I, 158 coal samples have been added to the Penn State/ERDA Sample Bank. Sixty-nine sets of analytical data and one characterized coal sample were provided upon request to other agencies.

Facet IV-A research on reactor development and operation shows that the gasification zone of a fuel bed is not diffusionally controlled. Pyrolysis of pulverized coal occurs under essentially isothermal conditions within the laminar flow furnace.

Methanol densities of chars, work on which has recently begun under Facet IV-B, are found to be quite similar to helium densities. Small angle x-ray scattering studies (Facet IV-B) show that the internal pore structure of coal chars changes with rank of the starting coal precursor and the maximum temperature at which the char is prepared.

Removal of inorganic impurities from chars by acid washing significantly reduces the extent of carbon deposition as a result of methane cracking. Reactivity and surface area are also affected by mineral matter removal. Furthermore, ion exchange increases char reactivity to steam.

Under Facet V-B, the addition of coal to water-oil emulsions has been found to increase the heat absorbed by the water load on the furnace to levels comparable to that of fuel oil no. 2.

TABLE OF CONTENTS

	Page
ABSTRACT	iii
OBJECTIVE AND SCOPE OF WORK	vi
TASK DESCRIPTIONS	vii
SUMMARY OF PROGRESS TO DATE	1
SAMPLE COLLECTION AND SEAM CHARACTERIZATION	4
Coal Sampling	4
Sampling Survey	4
COAL CHARACTERIZATION	6
Rapid Scan Automated Reflectance Microscope System	6
Hot Stage Microscopy	6
Coal Characterization	6
SAMPLE BANK OPERATION, MAINTENANCE, AND DEVELOPMENT	8
Service to Other Agencies	8
PENN STATE/ERDA COAL DATA BASE	9
Coal Data Base Activity Report	9
REACTOR DEVELOPMENT AND OPERATION	10
Evaluation of the Gasification Potential of Coals	10
Effect of Heating Rate and Soak Temperature on Volatile Matter Release	11
Characteristics of Chars Produced by Pyrolysis Following Rapid Heating of Pulverized Coal	12
COKES AND CHARS	19
Catalysis of Char Gasification	19
Methanol Densities of Coal Chars	21
Small Angle X-ray Studies on Coal Chars	25
Effect of Carbon Deposition on the Porosity and Reactivity of Chars	28
Reactivities of American Coal Chars in Steam	35
Reactivity of Ion Exchanged Lignite Chars to Steam	42
COMBUSTION OF CHARS AND LOW VOLATILE FUELS	46
Combustion of Char and Anthracite Coal in Large Utility Beds	46
COMBUSTION OF COAL-OIL EMULSIONS	52
Combustion of Coal-Oil-Water-Air Combustion Mixtures	52
CONCLUSIONS	56
REFERENCES	58

Page

CONTRIBUTORS 60

APPENDIX A
Kinetics of Gasification in a Combustion Pot: A Comparison of Theory and Experiment 61

OBJECTIVE AND SCOPE OF WORK

The primary objective of the overall program is to achieve the capability of predicting, from a knowledge of coal composition, the behavior of a coal in pre-conversion processing, coal gasification and coal liquefaction processes.

It is reasonable to ask if this goal is in fact attainable, recognizing the heterogeneity of coal seams. Clearly, it is not if one concerns oneself simply with the rank of the coal seam and its aggregate chemistry. A high volatile B coal from Indiana need not react to processing in the same manner as a high volatile B coal from Utah, even though their "chemistries" may be very similar. In contrast, a coal lithotype of a specific kind, at a given level of rank, can be expected to behave consistently, whether it derives from Alabama or Pennsylvania. Hence, the goal may very well be attainable if, as in the case of coal carbonization, we concern ourselves with the reacting entities and the properties of the important lithotypes.

The goal is to attain the same high level of predictive accuracy that is now found in the area of coal carbonization, where Penn State's collaborative work with the steel industry proved highly successful. To achieve this goal Penn State has devised an integrated program in which the success of the research is highly dependent on the effective operation of ALL of the program's Facets and Sub-facets which are as follows:

Facet I: Characterization of the Nation's Coal Resources
- I-A: Sample Collection and Seam Characterization
- I-B: Coal Characterization
- I-C: Sample Bank Operation, Maintenance and Development
- I-D: Penn State-ERDA Coal Data Base

Facet II: Coal Beneficiation and Pre-Use Processing

Facet IV: Significance of Coal Characteristics in Gasification Processes
- IV-A: Reactor Development and Operation
- IV-B: Cokes and Chars
- IV-D: Reactivity of Coal Chars
- IV-E: Catalysis Research
- IV-F: Differential Scanning Calorimetry

Facet V: Coal Combustion Research
- V-A: Combustion of Chars and Low Volatile Fuels
- V-B: Combustion of Coal-Oil Emulsions

THE CHARACTERISTICS OF AMERICAN COALS IN RELATION TO THEIR CONVERSION INTO CLEAN ENERGY FUELS

TASK DESCRIPTIONS

FACET I-A	Sample Collection and Seam Characterization
Task 1	Sampling Survey
Task 2	Sampling Plan
Task 3	Sampling
FACET I-B	Coal Characterization
Task 5	Characteristics and Use Potential of U. S. Coal Seams
Task 6	Characterization of Other ERDA Contractor Samples
Task 7	Automation of Microscopic Analytical Methods
FACET I-C	Sample Bank Operation, Maintenance and Development
Task 8	Maintenance of Coal Sample Bank
Tasks 9-14	Provision of Samples and Data to Penn State and Other Investigators
FACET I-D	Penn State/ERDA Coal Data Base
Task 15	Computerization of Data
Task 16	Evaluation of the Data Base
Task 17	Structuring and Utilization of the Data Base
FACET II	Coal Beneficiation and Pre-Use Processing
Task 18	Washability Characterization
Task 19	Physical Properties of Coal Lithotypes
Task 20	Techniques for Fractionation
Task 21	Beneficiation of Conversion Feedstocks
Task 22	Evaluation of Dry Flo Separator
FACET IV-A	Reactor Development and Operation
Task 23	Operation of Isothermal Furnace
Task 24	Pyrolysis of Coal Lithotypes
Task 25	Operation of Pressurized Isothermal Reactor
Task 26	Coal Reactivity
FACET IV-B	Cokes and Chars
Task 27	Effect of Variables on Char Structures
Task 28	Effect of Char Structures on Reactivities
Task 29	Catalytic Effect of Minerals in Gasification
Task 30	Effect of Catalytic Cations on Gasification
FACET IV-F	Differential Scanning Calorimetry
Task 31	DSC in Evaluating Coals for Conversion
FACET V-A	Combustion of Chars and Low Volatile Fuels
Task 32	Flame Ball Combustion Model
Task 33	Plane Flame Furnace
FACET V-B	Combustion of Coal - Oil Emulsions
Task 34	Combustion of Coal - Oil Emulsions

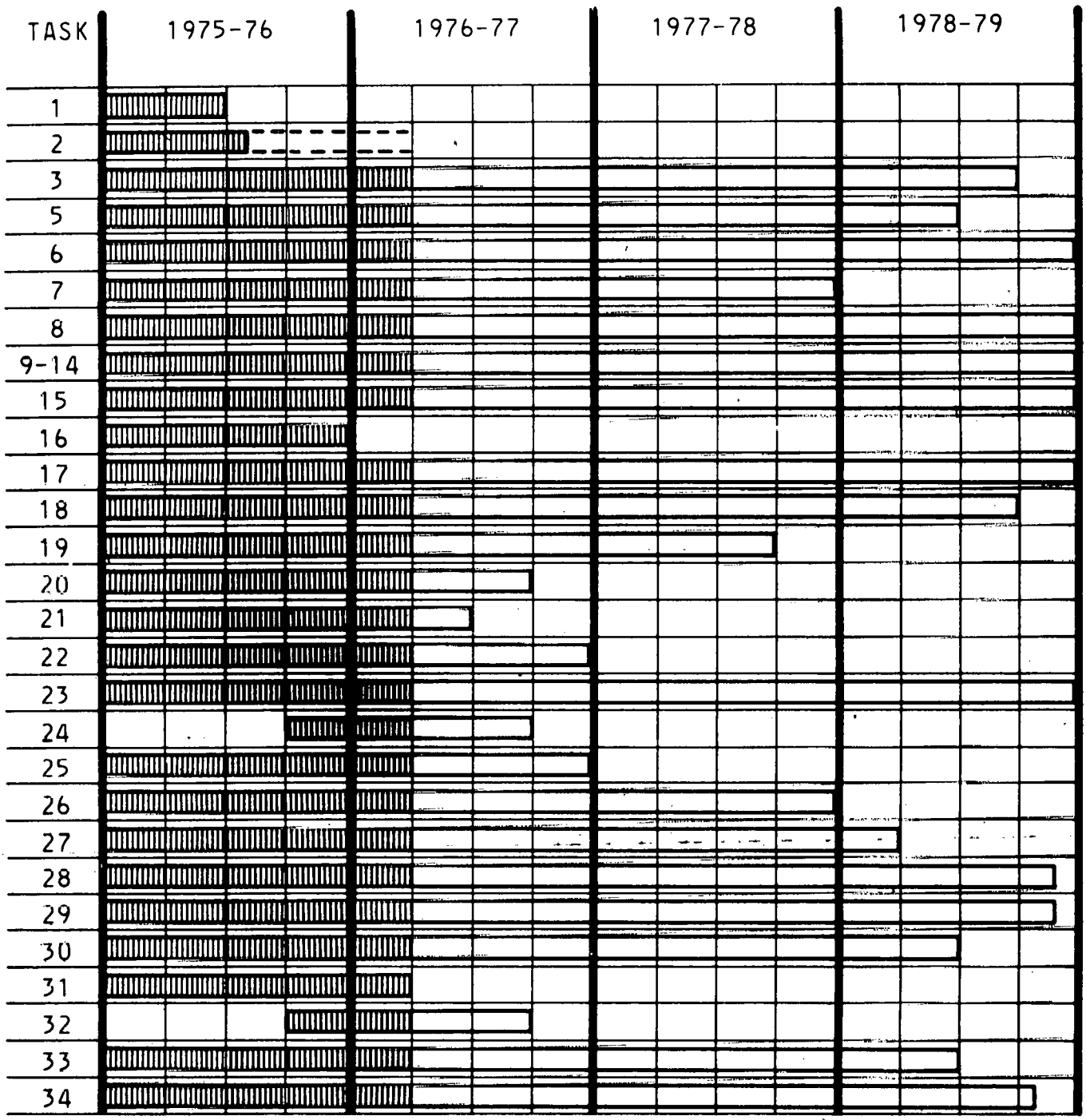

LEGEND

SCHEDULED

PROGRESS

SCHEDULE EXTENSION

EARLY START

PROJECT PLAN AND PROGRESS REPORT

Quarter Ending September 30, 1976

SUMMARY OF PROGRESS TO DATE

Sampling proceeded this quarter with the collection of 30 coal samples from Oklahoma and Texas. In addition, two drill cores were received from the Shell Oil Company. Sampling subcontracts with the University of Utah and Southern Illinois University have become effective; a total of 128 coal samples from 22 locations in five states have been received as a result of this program. Sixty-nine sets of analytical data and one characterized coal sample were provided upon request to other agencies engaged in coal research.

Work with the automated reflectance microscope system (Rapid Scan) continues to focus on the improvement of data interpretation. Hot-stage microscopy efforts have centered on the acquisition and installation of accessory equipment. Several interface items are still on order, until which time the system is not completely operable.

Expansion of the Penn State/ERDA Coal Data Base continued this quarter with the addition of data on 29 new coal samples, bringing the total number of coals in the data base to 336.

Facet II research on coal beneficiation and pre-use processing is on schedule with a sizable report being prepared for inclusion in the next quarterly technical progress report.

The design of the pressurized laminar-flow reactor of Facet IV-A is complete and construction is proceeding. A prototype coal-feeder has been successfully demonstrated and the design will be adopted.

The computer modeling program for coal particle pyrolysis has been completed and a special report is being prepared. The reactor system to be used for the 1000°C/sec pyrolysis study has been completed and is now being tested.

The rapid heating (of the order of 8×10^3°C/sec) of a North Dakota lignite (PSOC-246) is being studied using a laminar flow isothermal furnace. The effect of residence times up to about one second at maximum temperature (808°C) on changes in coal properties and weight loss has been studied. For residence times up to about one second the lignite is found to undergo a monotonic decrease in weight and a monotonic increase in surface area and denisty. Changes which the coal undergoes during the heating period are negligible compared to changes produced while at maximum temperature. The calculations supporting the experimental finding that pyrolysis during this heating period is negligibly small are the subject of this quarterly report.

Work has been initiated on the study of char gasification catalysis and methanol density of coal chars. In addition, study of the effect of carbon deposition on the porosity and reactivity of chars has commenced this quarter.

Small angle x-ray scattering (SAXS) is being used as a method of characterizing the pore structure of coal chars. Data have been collected for a series of chars prepared at temperatures ranging from 1050 to 1500°C. A primary parameter (ℓ_{III}-range of inhomogeneity) has been reported for each

sample. From a knowledge of the volume fraction of pores in the samples obtained from density data and this primary parameter, the pore structures of the chars have been defined in terms of surface area and characteristic dimensions of pores and matter between pores. Systematic variations are reported for all parameters with variations in rank of parent coal and heat treatment temperature.

Reactivities of 17, 40 x 100 mesh, U.S. chars prepared from coals of different rank by carbonization at 1000°C under controlled conditions have been measured at 910°C in one atmosphere of a nitrogen-steam mixture containing water vapor at a partial pressure of 17 torr. The lower rank coal chars are more reactive than those prepared from higher rank coal. A lignite char from Montana (PSOC-91) is about 260 times more reactive than a low volatile bituminous char from Pennsylvania (PSOC-127). Variation of reactivity with reaction temperature has been studied for PSOC-91 char.

As described in previous reports, three size fractions of a Darco, Texas lignite have been charred to 700°C, 800°C, and 900°C for the purpose of studying the reactivity of ion-exchanged lignite chars to steam. A similar series of chars have been prepared from the demineralized coal samples. Some work has been attempted on 48 x 60 and 60 x 100 mesh size fractions. However, steam requirements at the reaction temperatures being studied result in flow rates which cause poor mixing and heavy loss of fines leading to contradictory findings. The effect of particle size under reaction conditions studied is small. Ash and moisture contents, helium and mercury densities, size distributions, and carbon dioxide surface areas have been determined for all coals, chars, and reacted chars.

As a result of experimental difficulties encountered while studying the chemisorption of oxygen on Saran carbon, use of differential scanning calorimetry has been temporarily discontinued.

A large body of experimental results indicates that low to nearly zero volatile matter fuels (coal chars and anthracite coals) can be stabilized in a laboratory-scale combustion apparatus (the plane flame furnace). Order of magnitude shifts in the distance from the water-cooled inlet tube bank to the flame front can occur in switching from fuels suspected of having large accessible internal surface areas (macroporous) to fuels having little readily accessible internal surface area (microporous). Most of our work to date has been focused on the development of computer models to analyze and explain past experiments and to design future experiments. A model which considers only the stable combustion of a pulverized char flame in an infinite parallel plane geometry (properties varying only along direction of flow) is a logical and valid starting point toward further three dimensional modeling. The model permits examination of the detailed structure of pulverized char flames simply, yet realistically. Modifications to the model such as uneven nodal spacing, variable radiation absorption coefficient, and diffusional limitations on combustion rates are tending to make the results of the model closer to reality. Recently, the effects of the combustor length (between walls) and fuel reactivity have been investigated.

The combustion characteristics of coal-oil-water-air mixtures are being studied using a 2.0 million Btu/hr hot-wall type furnace with water tubes to simulate thermal loading. It has been found that the addition of water in

the fuel oil reduces the useful heat ouptut of the furnace; water addition also reduces the amount of excess air at various smoke levels, although the reduction of excess air at the smoke point (0% smoke) is not significant. The amount of soot particles produced was also reduced. Addition of coal to the oil-water-air emulsion greatly increases the heat output from the furnace to levels higher than those of fuel oil alone, without significant changes in the excess air requirements for complete combustion. The levels of soot emissions are comparable to that of fuel oil alone. In the course of this project over one hundred experiments have been performed.

FACET I-A: SAMPLE COLLECTION AND SEAM CHARACTERIZATION

COAL SAMPLING

During the period of this report a sampling trip was made to Oklahoma and Texas where nine coal seams were sampled. These include, from Oklahoma, a large channel sample of the Fort Scott seam (PSOC-399), a small channel sample of the Fort Scott seam from another pit (PSOC-400), a large channel from the Mineral seam (PSOC-401), a small channel sample of the Mineral seam from another pit about 1¼ miles away(PSOC-402). A large channel sample of the Stigler seam (PSOC-403) was collected, as were a large channel sample (PSOC-404) and three lithotypes (PSOC-405, 406, 407) of the Lower Hartshorne seam, and a channel sample (PSOC-408) and three lithotypes (PSOC-409, 410, and 411) of the Upper Hartshorne seam. Collected in Texas were a large channel sample (PSOC-412) and three lithotype samples (PSOC-413, 414, and 415) of the Darco Lignite, a large channel sample (PSOC-416) and three lithotypes (PSOC-417, 418, and 149) of a lignite seam near Winfield, Texas; a large channel sample (PSOC-420), three lithotypes (PSOC-421, 422, and 423), and a small channel sample about 0.2 miles from the large channel site (PSOC-424) of the Wildcat Lignite seam and a large channel sample (PSOC-425) and three lithotypes (PSOC-426, 427, and 428) from a lignite seam near Fairfield, Texas.

Two more drill cores of a bituminous coal from Maverick County, Texas were received from Shell Oil Company during this period. These cores will be used for some float-sink analyses and whatever other analyses the amount of material will allow.

Our sampling subcontracts with the University of Utah and Southern Illinois University became effective during this report period. We received 119 channel and lithotype samples, representing 20 different sites in Utah, Colorado, Wyoming, and Montana from the University of Utah sampling team. Southern Illinois University supplied us with nine samples from two different Iowa coal mines during this period.

SAMPLING SURVEY

A questionnaire was sent to 84 agencies to determine the extent to which the Nation's coals have been characterized. On the basis of 48 responses received to date a list of four tentative findings follows.

1) Of the 48 respondents, 17 routinely perform "minimal analyses" on their coals ("minimal analysis" is defined as proximate plus ultimate plus sulfur forms analyses).

2) Of the 17 agencies performing minimal analyses, 10 have more than 100 analyses on file.

3) Of the 24 state surveys responding, 21 indicated that 50 percent or less of our remaining reserves are characterized by minimal coal analyses.

4) Twenty-three agencies, including 16 state surveys, indicated that they would be willing to supply Penn State with coal samples. For the most part, these would be run-of-mine or channel samples.

FACET I-B: COAL CHARACTERIZATION

RAPID SCAN AUTOMATED REFLECTANCE MICROSCOPE SYSTEM

Work on the Rapid Scan (ARM) system has been primarily focused on data interpretation. A second suite of eleven coals with vitrinite contents of greater than 75 percent was scanned and the machine maximum reflectances were compared to the results obtained through manual analysis. The Rapid Scan values were found to be consistently lower. This is primarily due to the anisotropy of coal, which is known to increase with rank. In manual analysis, the microscope stage is rotated in order to obtain the maximum reflectance; whereas, the Rapid Scan records random reflectance values. Thus the deviation of Rapid Scan values from those obtained manually also increases with rank.

It appears, however, that once enough data have been accumulated, it will be possible to define a curve that will yield accurate results with the application of a weighted correction factor to neutralize the effects of increasing anisotropy.

Rapid Scan data output or reflectograms have also been studied in an effort to determine the relative percentages of maceral constituents. Two methods of fitting maceral distribution curves (Gaussian) have been applied.

Subsequent computer software modifications now allow the reflectograms to be broken into component parts by the subtraction of these curves. This also helps to define the input into the reflectogram of "edge" effects (coal-matrix interaction) and variance due to maceral interaction.

Future work will involve experimenting with high reflecting matrix material to minimize these "edge" effects. This will be an aid to the curve fitting process and lend to more accurate interpretation.

Research has begun on the feasibility of multi-spectral analysis with the Rapid Scan system.

HOT-STAGE MICROSCOPY

During this report period progress on the hot stage microscope has mostly been concerned with the acquisition and installation of equipment. The Leitz 1350 Heating Stage has been received and installed on the microscope. The necessary heating stage accessories have also been received. However, several interface items are still on order and hence the system is not yet completely operable.

COAL CHARACTERIZATION

Maceral analyses were completed on four PSOC samples (PSOC-399 through 402), seven samples supplied by other ERDA contractors (POC-292 through 298)

and on nine washability fractions from PSOC-317. Reflectance analyses were run on 30 new samples (PSOC-379 through 409), while 30 older samples were redone to check the pseudovitrinite reflectances. Maceral analyses under ultraviolet light were done on 18 samples (PSOC-385 through 393 and PSOC-395 through 403).

Samples of 130 coals collected before Fall, 1975, have been split out, prepared, and delivered to the Penn State Mineral Constitution Laboratory for major, minor, and trace elemental analyses and for mineralogic analyses during this quarter.

FACET I-C: SAMPLE BANK OPERATION, MAINTENANCE, AND DEVELOPMENT

SERVICE TO OTHER AGENCIES

Characterized coal samples and analytical data were provided by Penn State this quarter to agencies engaged in coal research as listed in Table 1.

Table 1. Coal Samples and Data Sent Out

Sample Number	Coal Sample	Coal Analysis	Organization	Research Interest
PSOC-24,81,82,85, 89,93,101,108,231 241,247,292		12	R.S. Datta, Syracuse Research Corporation	chemical comminution of coal
POC-116,122,148, 208,209 PSOC-22,24,86,88, 93,109,110,130,187, 190,216,220,223,239, 248,258,272,283,288, 294,314		26	C.Y. Wen, Department of Chemical Engineering West Virginia University	coal gasification
PSOC-55A,150,151, 152,250,309,310, 311		8	N. Vanderborgh, Los Alamos Scientific Laboratory	
PSOC-1,2,3,4,5,6, 187,217		8	B. Granoff, Sandia Labs.	autoclave hydroliquefaction
PSOC-89,101,124,126, 139,240a_3,240a_4,246		8	R. Musgrove, C.F. Braun & Co. Alhambra, CA	size reduction studies
PSOC-103,124,137,327, 330,331		6	P. Solomon, United Technologies Research Center	coal devolatilization
PSOC-190	1 lb	1	G. Gavalas, California Institute of Technology	pyrolysis
TOTAL	1	69		

FACET I-D: PENN STATE/ERDA COAL DATA BASE

COAL DATA BASE ACTIVITY REPORT

Expansion of the Penn State/ERDA Coal Data Base continued this quarter with the addition of data on 29 new coal samples, bringing the total number of coals in the data base to 336. Ninety-five trace element analyses and 80 major element analyses of coals already contained within the data base were incorporated into the existing computerized files.

Preliminary work has begun in the evaluation of the trace element, major element, and mineral analyses which are being generated on the coals contained within the Penn State/ERDA Coal Data Base. Computer facilities will be used to establish statistical relationships among these and other chemical, petrographic, and geologic data which are on file. Coals will be examined for overall chemical and geologic trends with respect to trace element, major element, and mineral matter distributions. Data correlations will also be investigated with respect to coal province and coal seam, with an attempt being made to quantify any relationships which may be found in the form of equations. Extensive use will be made of the statistical program packages available through The Pennsylvania State University Computation Center. Computer graphic facilities will be employed in plotting and mapping.

FACET IV-A: REACTOR DEVELOPMENT AND OPERATION

EVALUATION OF THE GASIFICATION POTENTIAL OF COALS

Introduction

The design of the pressurized laminar-flow isothermal reactor has now been completed by Autoclave Engineers, Inc. This includes a successful demonstration (under normal pressure) of a prototype screw coalfeeder, inclusion of an automatic hydrogen overflow shut-off loop, and compressor and valve rack modifications to permit outside installation. In addition to providing safer operation, the system modification may permit considerable savings to be realized in providing an acceptable building facility.

The result of an investigation by the University's industrial risk insurers has resulted in a decision that the Combustion Laboratory cannot house the reactor when it is used with hydrogen. Steps are being taken to acquire a satisfactory building facility for the reactor. If the ultimate needs are not satisfied by the time the reactor is delivered to the University, it will be installed at the Combustion Laboratory for conduct of the essential preliminary runs with non-explosive gases.

Experimental

The results of the Combustion Pot studied were reevaluated, and the contribution to the 16th International Combustion Symposium was revised. Entitled "Kinetics of Gasification in a Combustion Pot: A Comparison of Theory and Experiment", it is included as Appendix A to this report.

In order to reduce corrosion and the build up of slag in the combustion pot the existing insulating brick was replaced by Spartan 85 high aluminum brick with a bulk density of 2.77 g/cc. The use of the Spartan brick should decrease the frequency of replacement of the insulating brick. In addition to the two existing pressure taps (one in the airbox and one in the hood) four additional pressure taps were drilled on one side of the combustion pot. These taps will allow the pressure drop through the bed to be determined.

One hundred pounds of coke and 50 pounds each of three types of anthracite coal (PSOC-80, 81, and 85) were crushed and sized by hand. The capability of the Spartan brick to resist corrosion and slagging was investigated by running the combustion pot with both the coke and charcoal. It was found that the brick was very resistant to slag and corrosion. Cement was used to join the bricks in order to prevent air leakage. Two experiments were performed in order to determine whether the reaction in the combustion pot takes place internal to the particles or at their boundaries. The reaction was stopped prior to completion by removing the pot from under the exhaust hood and covering it with a steel plate. The bed was then removed in horizontal sections and the bulk and particle densities were measured. The results indicated that

the particle densities remained constant, thus leading to the conclusion that there is essentially no internal reaction. Additional experiments will be carried out to validate this result.

A computer model of the gasification reaction is in the process of being developed. Two tests were conducted to measure the pressure drop across the bed as inputs to the computer model.

The findings are that the combustion zone of a fuel bed is evidently diffusionally controlled, in agreement with past theories and conclusions; but the gasification zone is not, in disagreement with past theories. This last is considered to be the most significant finding, together with the estimate of the activation energy involved, of about 50 kcal. The practical significance of such a high temperature coefficient in a reactor is self-evident. What may also be new is the direct experimental evaluation or validation of the velocity and diameter functions in the combustion zone.

The activation energy of the carbon/carbon dioxide reaction in non-diffusional systems has, of course, been measured before, with values found in the range 25 to 80 kcal, which brackets our value[1]. Part of the variation is due to the difference between Zone I and Zone II measurements. Zone I behavior would, of course, show up as a drop in density, which was not observed. Zone II behavior at constant density implies that reaction is confined to a thin surface zone that is too thin to be detected by gross density changes; it would also mean that the true activation energy is closer to 100 kcal, which is high but not impossible.

The results also focus attention on the need for better information on a number of parameters if acceptable predictions are to be obtained from mathematical models of shaft reactors and in situ gasification. Factors of particular concern are: the internal surface area of the bed; the variation of bed porosity with particle size; the extent of internal reaction that is probably occurring in the gasification zone; and the behavior of the carbon monoxide kinetics in the bed.

EFFECT OF HEATING RATE AND SOAK TEMPERATURE ON VOLATILE MATTER RELEASE

Introduction

Variation in reported kinetic parameters for coal particle pyrolysis leads to speculation as to whether decomposition is in all cases occurring uniformly throughout the particle and at the reported particle temperatures. The question arises as to whether the pyrolytic reactions themselves, coupled with other characteristics such as particle size, play an important role in determining particle temperature profiles. Calculations have been made to determine theoretical particle temperature profiles with various values of thermal conductivity, heat reaction, and activation energy for different coal particle sizes. The results of the calculations indicate that under many of the experimental conditions assumed, particle temperatures and heating rates may be substantially in error.

Experimental

A coal particle pyrolysis computer program has been used to calculate conditions necessary to obtain true heating rates up to 1000°C/sec. The results of these calculations have been used in the design of a small pyrolysis reactor. The reactor has provisions for introducing milligram quantities of coal into a preheated chamber. Pyrolysis products from the reactor are transported to the analysis system by a carrier gas. Preliminary tests indicate the system is capable of achieving the desired heating rates.

The calculation of coal particle temperature profiles under pyrolysis conditions indicates that in many cases the pyrolysis reaction can act as a "heat sink" and introduce substantial temperature gradients within the particle. Under these conditions the main pyrolysis zone within the particle is undergoing reaction at a temperature different from the external temperature. Preliminary examination of published kinetic data indicates that many of the reported conflicts in rate mechanism can be ascribed to error in particle temperature assignment.

CHARACTERISTICS OF CHARS PRODUCED BY PYROLYSIS FOLLOWING RAPID HEATING OF PULVERIZED COAL

Introduction

Results from this investigation have led to the conclusion that pyrolysis of pulverized coal in the laminar flow furnace[2] occurs under essentially isothermal conditions. That is, pyrolysis during the heating and cooling periods in the furnace is negligibly small. The assumption of negligible pyrolysis during the cooling period is based on the experimental finding that the cooling rate of the pyrolysis products in the water-cooled collector probe is of the order of 2.7×10^4°C/sec. Calculations have been made which support the experimental finding that pyrolysis during the heating period is also negligible.

Experimental

The rate of gas (that is, volatiles) emission during pyrolysis can be expressed as a function of concentration[3]. That is,

$$dV/dt = k(V_0 - V) \qquad (1)$$

where k is the reaction rate constant, V_0 is the volume of gas liberated at the time $t = \infty$, and V is the volume of gas liberated at time t.

Assume that k can be expressed in an Arrhenius form as follows

$$k = k_0 \exp(-E/RT) \qquad (2)$$

where k_0 is the frequency factor, E is the activation energy, R is the gas constant, and T is the temperature.

Substituting Equation (2) in Equation (1) yields

$$dV/dt = k_o (V_o - V) \exp(-E/RT) \tag{3}$$

Assume that the heating rate (m) in the heating zone (Figure 1) is constant, that is,

$$dT/dt = m \tag{4}$$

Equation (3) can now be written as

$$dV/dt = (dV/dT)(dT/dt) = m(dV/dT) = k_o (V_o - V) \exp(-E/RT) \tag{5}$$

Separating the variables in Equation (5) gives

$$dV/(V_o - V) = (k_o/m) \exp(-E/RT)dT \tag{6}$$

which in integral form is

$$\int_0^V d\nu/(V_o - \nu) = \int_{T_o}^{T} (k_o/m) \exp(-E/R\tau)d\tau \tag{7}$$

or

$$\int_0^V d\nu/(V_o - \nu) = (k_o/m) \int_0^T \exp(-E/R\tau)d\tau - (k_o/m) \int_0^{T_o} \exp(-E/R\tau)\, d\tau \tag{8}$$

where ν and τ are the dummy variables, and T_o is the temperature at $t = 0$ (Figure 1).

Let $z = \tau/T$; at $\tau = 0$, $z = 0$; at $\tau = T$, $z = 1$; $dz = (1/T)d\tau$.

Substituting these quantities into Equation (8) yields

$$\int_0^V d\nu/(V_o - \nu) = (k_o T/m) \int_0^1 \exp[-(E/RT)/z]dz - (k_o T_o/m) \int_0^1 \exp[-(E/RT_o)/z]dz \tag{9}$$

The two integrals on the right hand side can be expressed in the form of the exponential integral of order 2, where the exponential integral of the nth order is defined by[4]

$$E_n(x) = \int_0^1 \mu^{n-2} \exp(-x/\mu)d\mu \tag{10}$$

Integrating Equation (9) gives

$$-\ln (V_o - V)/V_o = (k_o T/m) E_2(E/RT) - (k_o T_o/m) E_2(E/RT_o) \tag{11}$$

which can be rearranged to

$$(V/V_o) = 1 - \exp \{ -[(k_o T/m)E_2(E/RT) - (k_o T_o/m)E_2(E/RT_o)] \} \tag{12}$$

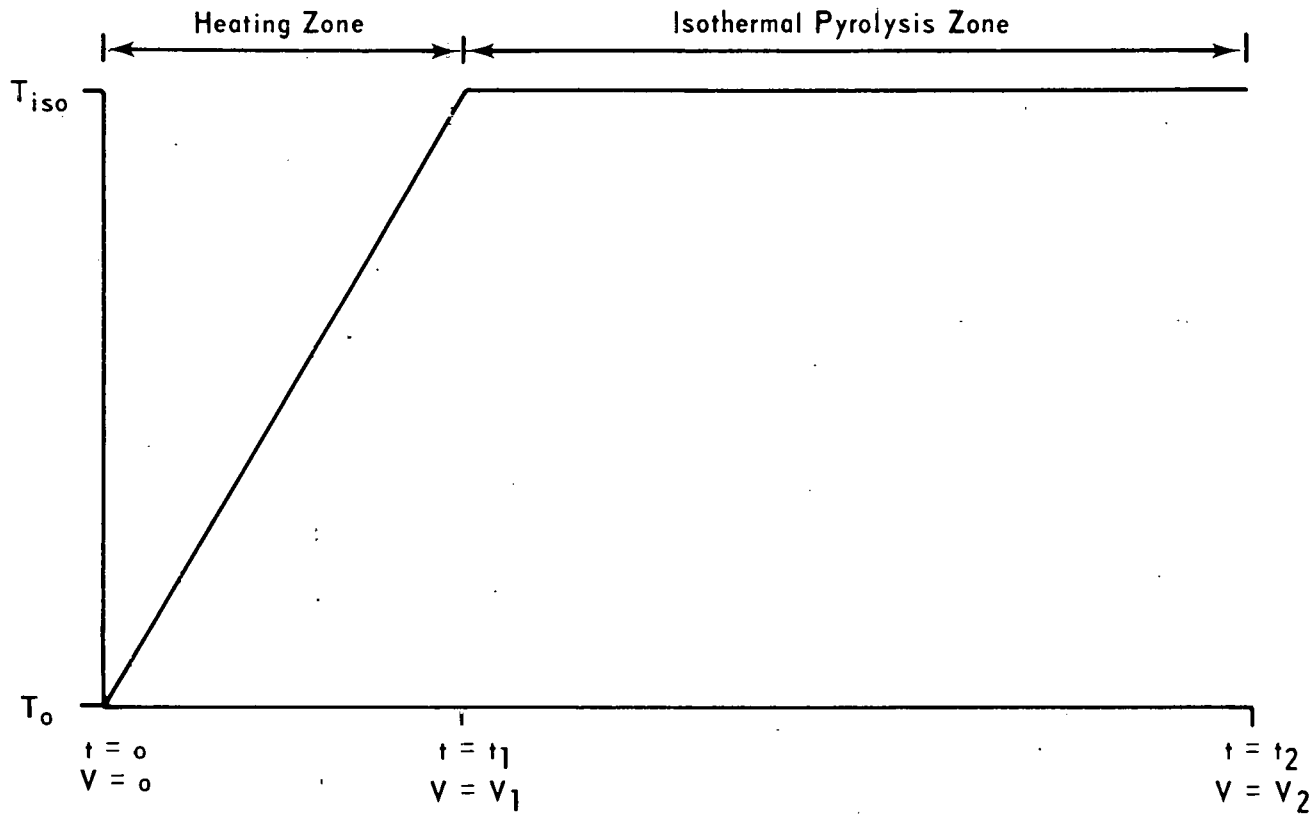

Figure 1. ASSUMED TEMPERATURE PROFILE OF COAL PARTICLES IN THE HEATING AND PYROLYSIS ZONES OF THE FURNACE

For large values of x there is an asymptotic expansion of the exponential integral[4] given by Equation (10), that is,

$$E_n(x) = (1/x)\, e^{-x} [1 - n/x + n(n+1)/x^2 + \ldots] \qquad (13)$$

Thus, $E_2(E/RT)$ and $E_2(E/RT_o)$ in Equation (12) can be evaluated as $(e^{-E/RT})/(E/RT)$ and $(e^{-E/RT_o})/(E/RT_o)$ respectively to quite an acceptable accuracy.

Equation (4) can be rearranged and expressed in an integral form as follows

$$\int_{T_o}^{T} dT = m \int_{0}^{t} dt \qquad (14)$$

Integrating this equation yields

$$T = T_o + mt \qquad (15)$$

where $T_o = 300°K$.

Substituting Equation (15) into Equation (12) gives

$$(V/V_o) = 1 - \exp \left\{ -[k_o/m)(T_o+mt)\, E_2(E/R(T_o+mt)) - (k_oT_o/m)E_2(E/RT_o)] \right\} \qquad (16)$$

where $0 \leq t \leq$ (Figure 1).

At $t = t_1$, $V = V_1$ where V_1 is the quantity of gas evolved during the heating period from $t = 0$ to $t = t_1$ under conditions of a linear temperature rise with time.

In the isothermal pyrolysis zone (Figure 1, case $t_1 < t < t_2$) Equation (3) can be expressed in an integral form as

$$\int_{V_1}^{V} d\nu/(V_o - \nu) = \int_{t_1}^{t} k_o \exp(-E/RT_{iso})dt \qquad (17)$$

which, upon integration, gives

$$-\ln[(V_o - V)/(V_o - V_1)] = k_o\, (t - t_1) \exp(-E/RT_{iso}) \qquad (18)$$

Equation (18) can be rearranged to

$$(V/V_o) = 1 - (1 - V_1/V_o) \exp[-k_o\, (t - t_1) \exp(-E/RT_{iso})] \qquad (19)$$

In Equation (19), when $t = t_1$, $V/V_o = V_1/V_o$ or $V = V_1$; when $t = \infty$, $V/V_o = 1$ or $V = V_o$.

Classical unimolecular theory predicts[5] a value of the frequency factor (k_o) of the order 10^{13} sec^{-1}. Substituting the values of k, k_o, R, and T into Equation (2) gives, after rearrangement, a value of the activation energy (E).

For example, when $k = 2.64\ sec^{-1}$ and $T = 1081°K$ (this investigation), $E \simeq 63$ kcal/mole.

Equation (16) can now be used to calculate the fractional weight loss of volatiles (V/V_0) in the heating zone, where $0 \leq t \leq t_1$. At $t = t_1$, a value of V_1/V_0 is obtained. This value is then substituted into Equation (19), and the fractional weight loss of volatiles in the isothermal pyrolysis zone can be determined. In this investigation $t_1 = 0.095$ sec (heating time) and $t_2 = 0.3$ (maximum residence time of particles in the heating and isothermal pyrolysis zones).

The results from this calculation are presented in Figure 2. They show a variation of the fractional weight loss of volatiles (V/V_0) with time, with $k_0 = 10^{13}\ sec^{-1}$ and $E = 40$-63 kcal/mole. It is clear from Figure 2 that the fractional weight loss of volatiles during the heating period is negligibly small (<2%) for all values of $E > 55$ kcal/mole. If one accepts the value of $10^{13}\ sec^{-1}$ for k_0 which, in this investigation, gives a value of $\simeq 63$ kcal/mole for E, then the results in Figure 2 are consistent with the conclusion that pyrolysis during the heating period is negligibly small. Figure 2 shows, however, that the fractional weight loss of volatiles during the heating period is large for all the values of $E < 55$ kcal/mole. For example, when $E = 50$ kcal/mole, pyrolysis occurs almost entirely during the heating period.

Since it is unlikely that k_0 would necessarily remain constant when E varies, it is of interest to make a calculation in which the value of $\alpha = V_1/V_0$ is assumed, and then the variation of k_0 with E is determined. Substituting α into Equation (16) gives, after rearrangement

$$k_0 = \ln(1 - \alpha)/[(T_{iso}/m)E_2(E/RT_{iso}) - (T_0/m)E_2(E/RT_0)] \qquad (20)$$

where $T_{iso} = T_0 + mt_1$.

The variation of k_0 with E has been determined (Figure 3) when $\alpha = 0.01$, 0.05, or 0.10; that is, when 1, 5, or 10 percent of weight loss of volatiles occurs during the heating period. For example, Figure 3 shows that if the fractional weight loss of gas in the heating zone is 1 percent then the frequency factor (k_0) has to be in the range 10^{12} to $10^{14}\ sec^{-1}$ for the activation energy (E) to be in the range of 60-65 kcal/mole. This is consistent with the results presented above.

The next quarter will be spent studying the characteristics of the North Dakota lignite (PSOC-246) chars obtained from the laminar flow isothermal furnace in the presence of a gaseous medium other than nitrogen.

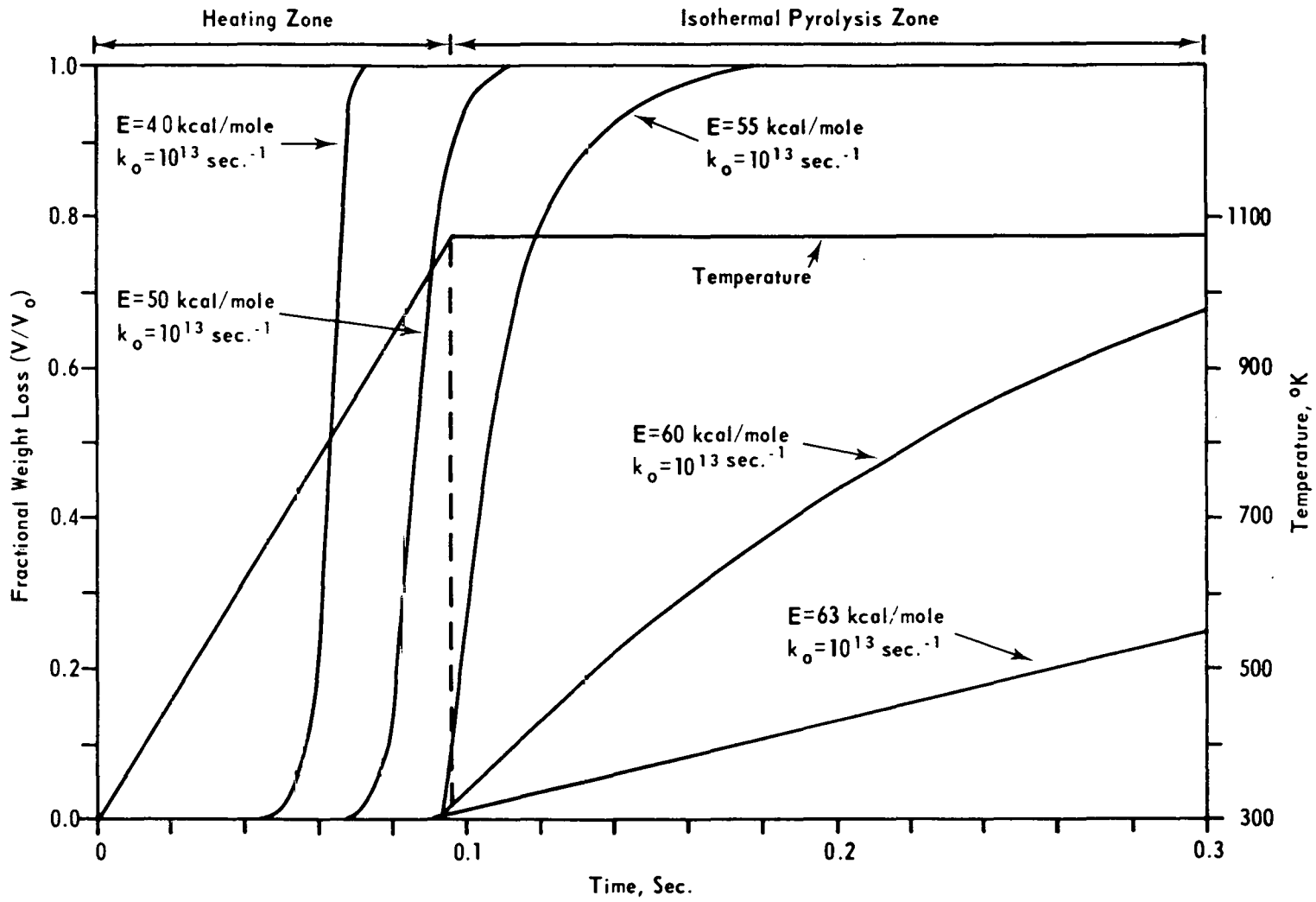

Figure 2. VARIATION OF FRACTIONAL WEIGHT LOSS OF VOLATILES (V/V_0) WITH TIME (Calculated from Equations (16 & 19))

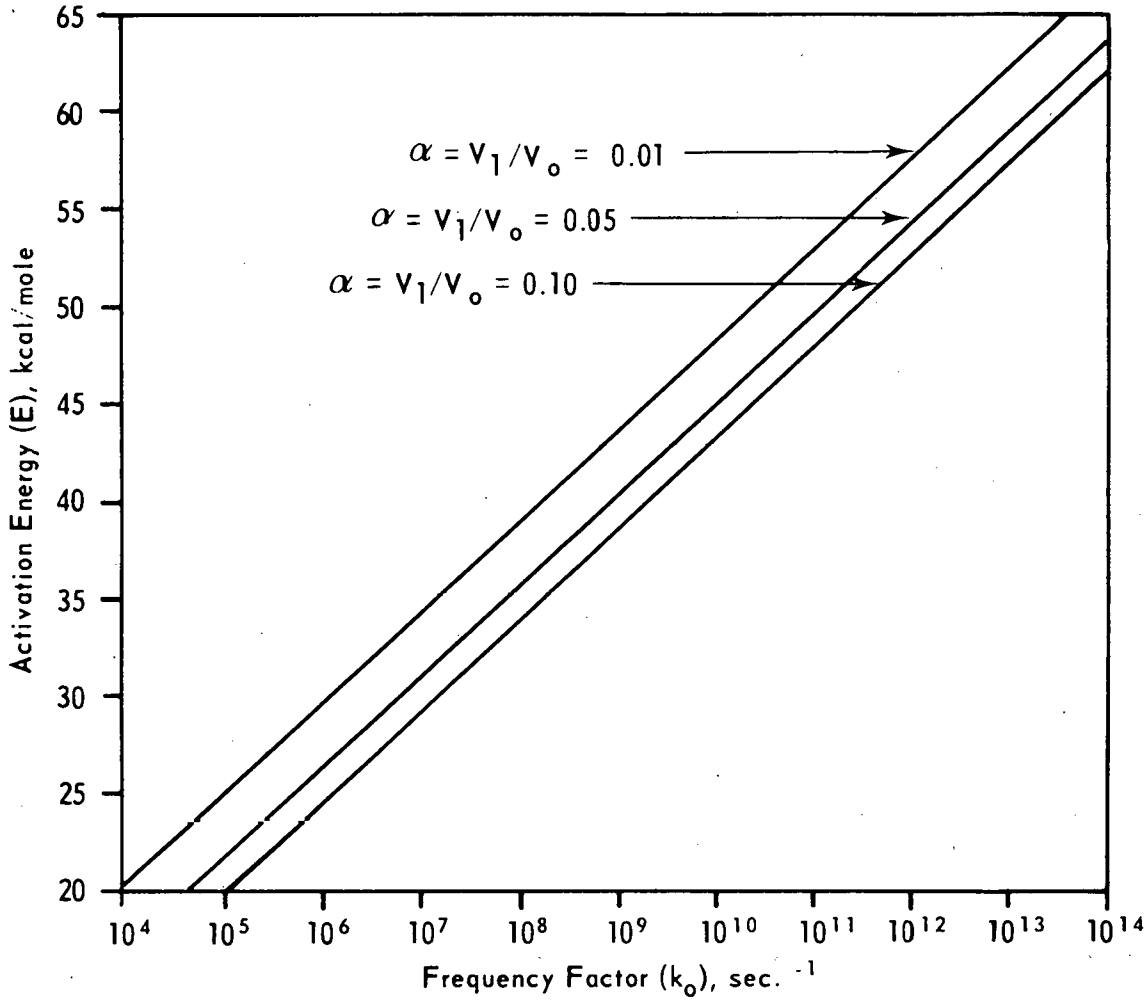

Figure 3. VARIATION OF THE FREQUENCY FACTOR WITH THE ACTIVATION ENERGY FOR A GIVEN VALUE OF $\alpha (= V_1/V_0)$ AT THE END OF THE HEATING PERIOD

(Calculated from Equation (20))

FACET IV-B: COKES AND CHARS

CATALYSIS OF CHAR GASIFICATION

Introduction

Work has been initiated to study the reactivity in air of Saran carbon as a function of platinum loading and degree of its dispersion. This report describes the experimental procedure for impregnating Saran carbon with chloroplatinic acid. Reasons for lack of reproducibility have been discussed. The objective of this study is to ultimately gain a better understanding of catalysis of coal char gasification reactions.

It is well known that chars derived from lignites are highly reactive during gasification. Lignites are associated with considerable amounts of carboxylic acid groups. It is possible that protons of the carboxylic acid groups may have undergone ion exchange with cations, such as Na^+, K^+, and Ca^{++} as a result of extended contact of embedded coals with ground water. It is likely that following decarboxylation (during the carbonization process) the cations are converted to metals or metal oxides which are dispersed on the char surface in the form of very fine particles. This could account for the high reactivity of lignite coals during gasification. It would be desirable to study the effect of catalyst loading and of degree of its dispersion (ratio of surface metal atoms to the total number of metal atoms) upon reactivity of coal chars. However, in the case of metal cations which are normally present in lignites no reliable methods are known for measuring their degree of dispersion. There is thus a need to use a metal for which a method of determining its degree of dispersion is well known. Furthermore, since coals and, hence, chars are invariably associated with catalytic inorganic impurities, it is desirable to use a char support similar in structure but purer than lignite.

The metal catalyst chosen for this study was platinum. Bartholomew and Boudart[6] have suggested a technique for determining the degree of dispersion of supported platinum. The char support used in the present study was prepared by carbonizing (at 900°C) Saran, which is a copolymer of polyvinylidene chloride and polyvinyl chloride in the ratio of about 9:1. Saran char is highly microporous in nature and has a structure similar to lignite chars.

Dacey and Thomas[7] and Barton and others[8] have shown that Saran char has a uniform array of slit-shaped micropores of 5.5 to 6Å in width. It is quite possible that chloroplatinic acid, which has a minimum dimension of about 7Å, may not penetrate into the Saran char pore structure. It will thus be desirable to determine the degree of dispersion of platinum on Saran char activated to different levels of carbon burn-off. It has been recently reported from this laboratory[9] that in the case of a homogeneous graphitized carbon black, the degree of dispersion of platinum, for a given amount of catalyst loading, increases with increase in the extent of prior activation (gasification) of the sample. The increase has been attributed to an increase in surface heterogeneity.

It has been suggested that gasification increases the magnitude and/or frequency of the potential energy barriers for the diffusion of platinum species across the surface, thus hindering particle growth. However, in the case of turbostratic Saran char which is initially heterogeneous, gasification is expected to have only a slight effect on surface heterogeneity. Instead, gasification is expected to enlarge pore size which will result in a more efficient infiltration of chloroplatinic acid into the internal pore structure. Expressed in other words, an increase in degree of dispersion (for a given catalyst loading) upon gasification of Saran char will probably be indicative of an increase in porosity rather than an increase in surface heterogeneity of the carbon.

The aim of the present study is to investigate systematically the effect of platinum loading and degree of its dispersion on reactivity to air of Saran carbon activated to different levels of carbon burn-off. This report describes the preliminary results of such an investigation.

Experimental

Saran was carbonized at 900°C by Airco Speer Carbon Products. It was then ground by hand using a ceramic mortar and pestle. The 70 x 100 mesh (U.S. standard series) fraction was separated and used in this study. The experimental procedure for the preparation of supported platinum was essentially the same as that described by Bartholomew and Boudart[6]. The procedure consists of mixing a known weight of carbon with a solution containing a known amount of chloroplatinic acid dissolved in a 4:1 volume mixture of benzene and absolute ethanol (50 ml of mixture per g of carbon). The suspension was mechanically stirred and evaporated to near dryness at ambient temperature by bubbling nitrogen through the suspension for 12 hr. After further drying the mixture in a vacuum oven at 70°C overnight, it was reduced in flowing ultra-pure hydrogen (20-30 cc/min) at 500°C for 10 hr.

The degree of dispersion of platinum was determined by using the titration technique suggested by Benson and Boudart[10]. For this purpose, a 2-3 g portion of the reduced sample was evacuated and heated at 110°C for 1 hr. The sample was then oxidized under approximately one atmosphere of ultra-pure oxygen at 25°C for 1 hr. The sample was then evacuated for 5 hr and a known amount of ultra-pure hydrogen admitted. The amount of hydrogen adsorbed on the oxidized sample was determined at 25°C.

The following stoichiometry was used to determine the number of platinum atoms at the surface:

$$Pt(O) + \frac{3}{2} H_2 \rightarrow Pt(H) + H_2O \qquad (21)$$

This stoichiometry requires that all water vapor released during the titration be completely adsorbed by the support. For this purpose about 0.5 g of Drierite was mixed with the platinum-carbon sample before the titration. Adsorption of hydrogen on Drierite is negligible.

In order to study the effect of activation of Saran char to different levels of carbon burn-off on degree of dispersion of platinum, it was essential

to have the same platinum loading on the char. Chloroplatinic acid cannot be obtained by direct weighing. In order to circumvent this difficulty, a stock solution of chloroplatinic acid in ethanol was prepared. Platinum concentration in the solution was determined gravimetrically. For impregnating char samples, an aliquot of the stock solution was diluted with benzene and ethanol to obtain a desired concentration of platinum.

Hydrogen consumption (25°C) on platinum supported on Saran char for duplicate runs A and B for the same catalyst loading are plotted in Figure 4. The volume of hydrogen uptake was estimated by extrapolating the isotherms to zero pressure. The intercept in each case represents the extent of hydrogen uptake. The two plots, A and B, do not superimpose on each other. Moreover, the degree of dispersion of platinum in runs A and B are not the same, being 82.4 and 87.1 percent, respectively. The observed lack of reproducibility is thought to be due to non-uniform impregnation of char particles. During the preparation of the impregnated sample, a magnetic stirrer is used to agitate the suspension. It was observed that when the volume of solution decreased due to evaporation the stirrer tended to stack char particles on the sides of the beaker so that the particles within the solution were impregnated with a higher concentration of solution than the char particles stacked on the sides of the beaker. This resulted in an uneven impregnation of the char particles. To overcome this difficulty in the future, the stirrer will be removed while enough solution is still left to cover all the char particles. The remaining solution will be evaporated under vacuum.

In order to have optimum conditions for impregnation of carbon with chloroplatinic acid, 1 g portions of Saran carbon will be treated with chloroplatinic acid (corresponding to one percent by weight platinum loading) for different intervals of time. An aliquot of each sample will be examined spectrophotometrically for a decrease in the concentration of chloroplatinic acid in the solution. In subsequent experiments carbon will be kept in contact with the chloroplatinic acid solution for a time which corresponds to a maximum uptake of chloroplatinic acid.

Saran carbons will be loaded with 0.5, 1, 2, and 5 weight percent platinum and degrees of dispersion will be determined as a function of catalyst loading.

In order to study the effect of prior activation (burn-off) of Saran carbon on degree of dispersion of platinum, Saran carbon will be activated in carbon dioxide to different levels of carbon burn-off (in the range 5-40%). Surface areas of various samples will be determined. Each sample will be loaded with 1 weight percent platinum.

METHANOL DENSITIES OF COAL CHARS

Introduction

True and apparent densities of coals and chars are conventionally determined by the displacement of helium and mercury, respectively. These densities are useful in the physical characterization of coals and chars. However,

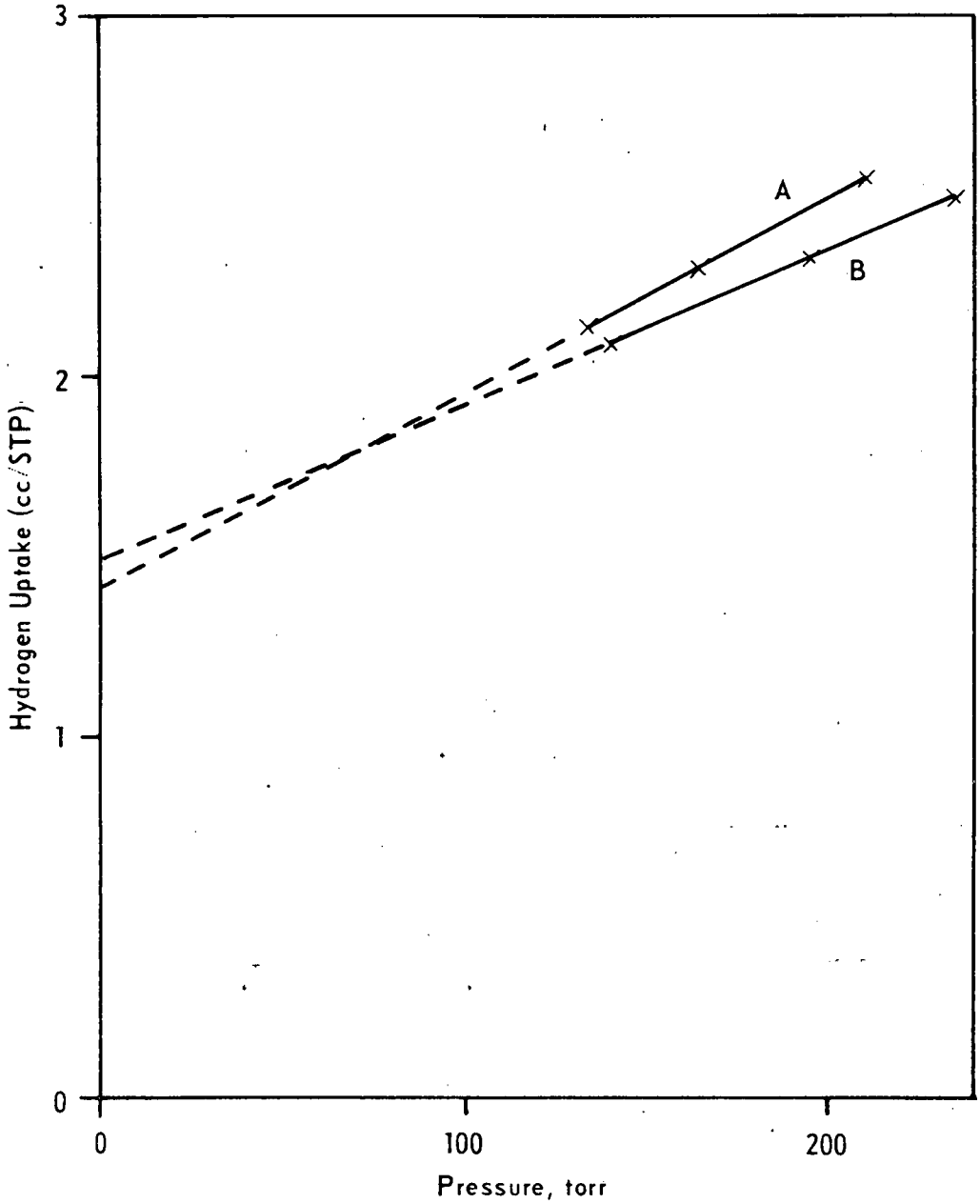

Figure 4. HYDROGEN UPTAKE AT 25 °C DURING TITRATION OF PLATINUM SUPPORTED ON SARAN CHAR

determination of helium densities needs an elaborate vacuum system and the experimental procedure is cumbersome and time consuming. Various workers have suggested the use of different fluids to determine the densities of coals. Perhaps methanol has been used most in such studies. However, methanol densities of coals suffer from the drawback that coals imbibe methanol. Therefore, such densities cannot be considered to be 'true' densities of coals. However, when coals are carbonized at higher temperatures, the resultant chars are not expected to imbibe any methanol. The aim of the present study is to investigate if methanol densities of chars are comparable to the helium densities.

Experimental

A North Dakota lignite coal (PSOC-87) was used for the preparation of char. About 30 g portions of 40 x 100 mesh coal was carbonized at 855 to 1000°C in a tube furnace. The heating rate used was 10°C/min. Soak time at maximum temperature was 2 hr. During heat treatment, a stream of prepurified nitrogen was passed continuously over the sample.

About 4 g of char were taken in a graphite boat which was placed in a tube furnace. The system was purged with prepurified nitrogen for 1 hr. Heating was then started at a rate of 10°C/min. The sample temperature was raised to 855°C. Soak time at this temperature was 1 hr. Following this, nitrogen was replaced by a mixture of methane and nitrogen at 1 atm pressure, containing methane at a partial pressure of 50 torr. The extent of carbon deposition (CD) was estimated from the weight increase of the sample after the reaction.

The raw and carbon deposited char samples were activated to different levels of carbon burn-off in air at 375°C.

Helium densities were determined in the manner described previously[11]. Methanol densities at 25°C were determined using conventional pycnometers. For each sample methanol densities (in duplicate) were determined after different intervals of contact time.

Helium and methanol densities of various samples are listed in Table 2. Reproducibility of the data for duplicate runs is reasonably good. The methanol densities show a drift with time. This behavior has been observed previously and is characteristic of microporous adsorbents. It is noteworthy that methanol densities after about 72 hr contact time are, in general, fairly close to the helium densities. In no case do methanol and helium densities for a given sample differ from each other by more than 5 percent. These results suggest that methanol densities of chars can be used as a measure of their true densities. The distinct advantage of methanol densities is that a number of determinations can be made simultaneously. In contrast, it takes at least two days for each helium density measurement.

Densities of chars in water will be reported in the next quarterly report. It is expected that densities in water will be comparable to the helium and methanol densities.

Table 2. Helium and Methanol Densities of Chars

Sample		Helium Density g/cm^3 (mmcb)	Methanol Densities g/cm^3 (mmcb) After 2 hr		24 hr		48 hr		72 hr		96 hr		120 hr		192 hr	
			1	2	1	2	1	2	1	2	1	2	1	2	1	2
	CD %(daf)								CD Series							
855°C Char	0	2.11	1.73	1.70	1.99	1.92	2.09	2.02	2.12	2.05	2.12	2.08	2.12	2.07	-	-
	1.0	1.90	1.88	1.95	2.03	2.06	2.05	2.07	2.08	2.08	2.08	2.09	-	-	-	-
	1.7	2.01	1.94	1.86	2.07	1.99	2.09	2.02	2.11	2.04	2.11	2.05	-	-	-	-
	2.6	1.88	1.75	1.84	1.80	1.89	1.83	1.91	1.84	1.91	1.85	1.94	1.85	1.91	-	-
1000°C Char	0	2.12	2.03	1.98	2.06	2.02	2.10	2.07	2.12	2.09	2.13	2.10	2.13	2.09	-	-
	3.6	2.04	1.89	1.86	1.94	1.91	1.97	1.94	2.04	2.02	2.05	2.05	2.05	2.04	-	-
	Burn-off %(daf)								Burn-off Series							
855°C Char	0	2.11	1.73	1.70	1.99	1.92	2.09	2.02	2.12	2.05	2.12	2.08	2.12	2.07	-	-
	1.1	2.07	1.87	1.91	2.04	2.02	2.06	2.05	2.10	2.08	2.11	2.06	-	-	2.11	2.10
	2.3	2.07	1.93	1.99	2.01	2.07	2.04	2.09	-	-	-	-	2.10	2.14	2.10	2.12
	10.2	2.16	1.91	1.95	2.04	2.08	2.07	2.06	2.10	2.08	2.16	2.16	2.13	2.14	2.14	2.14
	33.6	2.17	2.07	2.06	2.17	2.16	2.17	2.18	2.17	2.19	2.18	2.19	2.18	2.18	2.17	2.17
855°C Char 2.6% CD	0	1.88	1.75	1.84	1.80	1.89	1.83	1.91	1.84	1.91	1.85	1.91	1.85	1.91	-	-
	1.7	2.04	1.61	1.64	1.74	1.82	-	-	1.87	1.96	2.01	2.06	2.02	2.05	-	-
	3.7	2.00	1.79	1.69	1.99	1.89	2.02	1.97	2.02	2.01	2.04	2.06	2.05	2.07	2.06	2.07
	29.1	2.06	1.95	1.87	2.00	1.96	2.02	2.03	2.07	2.03	2.03	2.03	2.02	2.04	-	-

SMALL ANGLE X-RAY STUDIES ON COAL CHARS

Introduction

Conventional methods of characterizing pore structures of coal chars are somewhat limited for chars prepared at temperatures in excess of 1000°C. The reason being that for these types of materials, the cavity/aperture pore systems limit the penetration of probing fluids. Hence, surface areas are grossly underestimated. On the other hand, it is known from densities in mercury and helium that these samples contain extensive porosity. Certain parameters defined by SAXS do not suffer from such limitations.

Previously, we have described in detail the theoretical background for the interpretation of SAXS data and reported values of a primary parameter obtained for a series of chars. The parameter reported, 'ℓ_m' (range of inhomogeneity), is a measure of both a characteristic length of pores and characteristic length of solid material between pores. Figure 5 is an idealized representation of a porous two phase solid. The chords intersecting the pore/solid system are representative of the SAXS parameters. An average of all intercepts through the pores is defined at d_{voids}, the average of intercepts through the solid is defined at d_{matter}. The primary parameter ℓ_m is given by Equation (22), showing it to be a 'reduced' distance. In the representation

$$\frac{1}{\ell_m} = \frac{1}{d_{voids}} + \frac{1}{d_{matter}} \qquad (22)$$

in Figure 5 it should be noted that it is the inverse of a real system in that this portrays a series of random x-ray beams intersecting a defined pore/solid system whereas in the real situation we have a random pore system intersected by a single beam.

The parameters d_{void}, d_{matter} and surface area per gram (interface area between pores and solid matrix) are derived from ℓ_m by the following relationships involving the volume fraction of voids within the carbonaceous matrix-'C'.

$$d_{voids}\ (A) = \ell_m/(1-C) \qquad (23)$$

$$d_{matter}\ (A) = \ell_m/C \qquad (24)$$

$$SA/g\ (m^2/g) = KC(1-C)/\ell_m \qquad (25)$$

The constant K is given by $4 \times 10^4/\rho_{Hg}$, where ρ_{Hg} is the density of the solid in mercury.

Experimental

Values of ℓ_m obtained for the char samples are plotted in Figure 6 (reported previously); they have been plotted versus percent C (daf) of the parent coal. All the parent coals were demineralized with hydrochloric/hydroflouric acid before carbonization in nitrogen. For the 1050°C chars

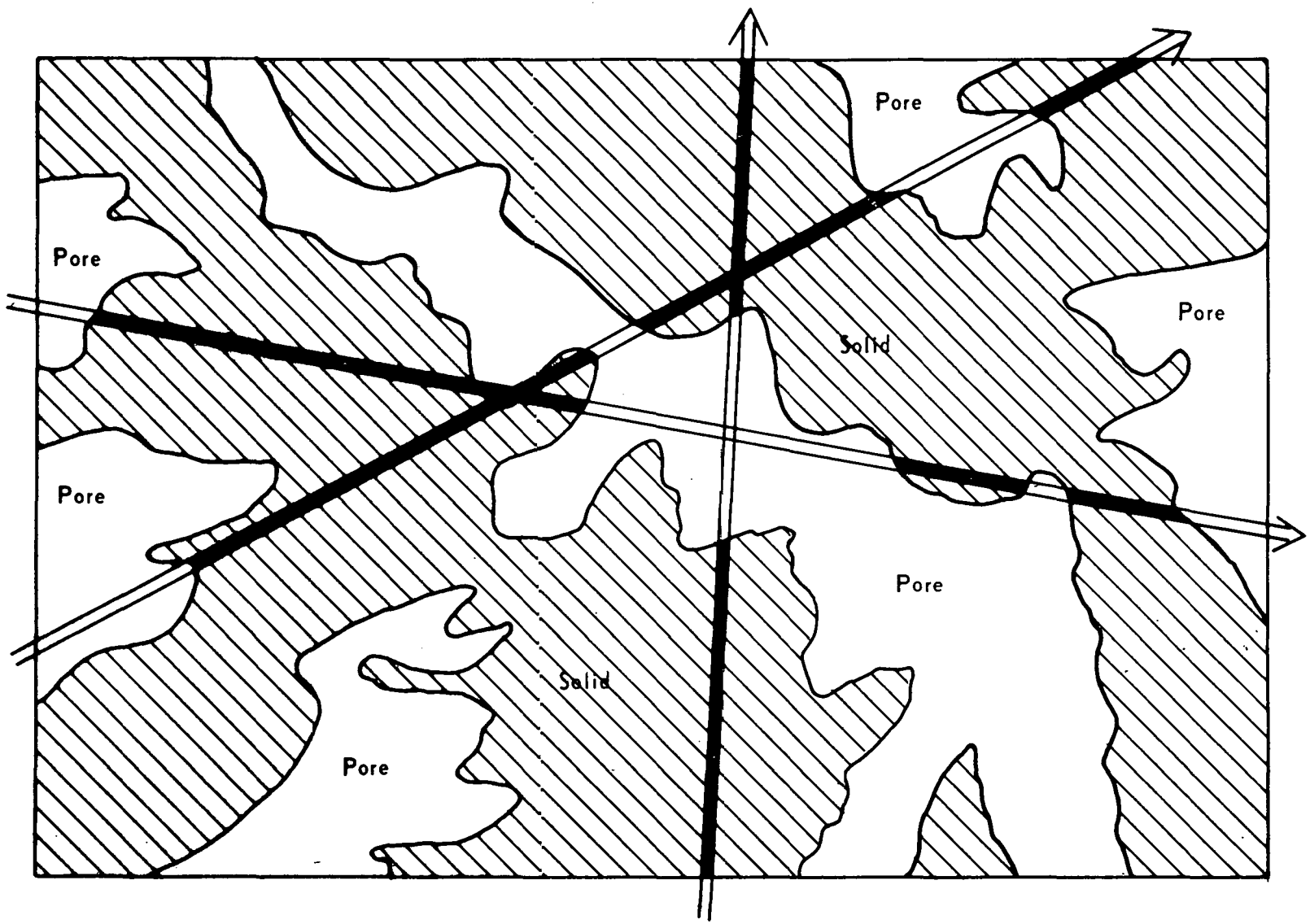

Figure 5. IDEALIZED REPRESENTATION OF PORE/SOLID SYSTEM AND INTERSECTING X-RAY BEAMS

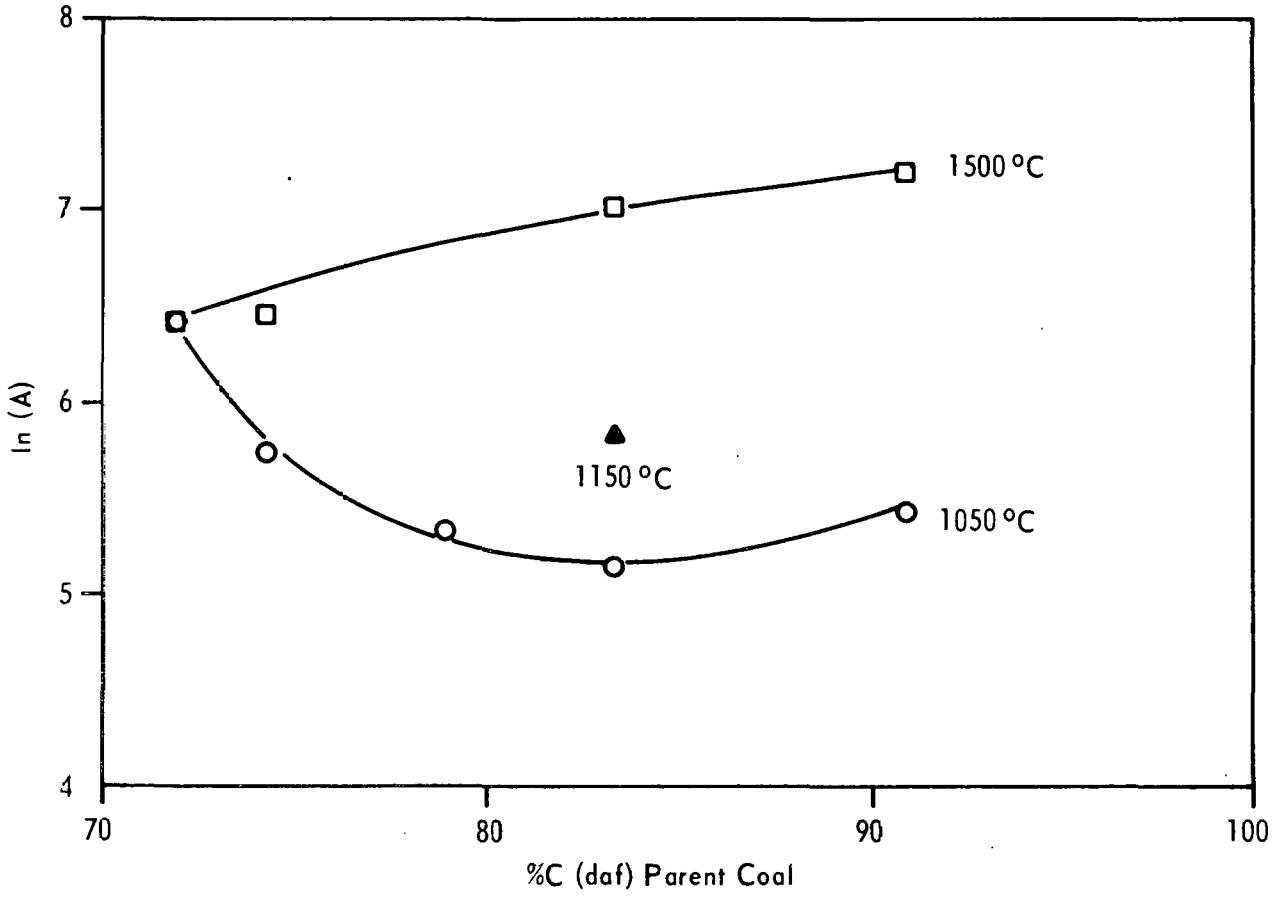

Figure 6. VARIATION OF LN WITH CARBON CONTENT OF PARENT COAL

there is a systematic variation with rank of parent coal. However, it will be noted that values of ℓ_m for the 1500°C are all quite similar for these samples. The value of the one 1150°C sample falls between the two other curves.

Figures 7, 8, and 9are plots of the secondary parameters, d_{void}, d_{matter} and surface area versus percent C (daf) of the parent coals. These data were obtained by estimating the value of 'C' (vol fraction of pores) from density data (that is, $C - 1 - \rho_{Hg}/\rho_x$, where ρ_{Hg} and ρ_x are the densities as measured by mercury and x-ray diffraction respectively). In the last report we described how this procedure for estimating C can overestimate its value. To some extent, some of these values are unrealistic because the envelope density as measured by mercury density is a function of the very large pores which do not contribute much to the SAXS profile. The errors will be the greatest for the low rank coal chars, since they contain the greatest concentration of large pores. However, it is considered that the values determined by this procedure are of value. At a later date we will compare them with those found from 'absolute intensity data'. To obtain such data we require an intensity standard; such a standard is on order and is expected in the near future.

In Figure 7 it can be seen that the chars produced at 1050°C show the greatest change with rank of parent coal. However, the values of d_{voids} for the 1500°C series are remarkably similar. It will be noted that the 'average pore size' of all chars lies between 10A and 6.7A. As heat treatment increases, the size generally increases, the exception being the char produced from the lowest rank coal. Similar results are reported for a series of 'glassy carbons'[12]. Values of d_{matter} show (Figure 8) an increase with rank of parent coal and with heat treatment temperature. It is suggested that this observation reflects the increase in order within the carbonaceous matrix.

Finally, inspection of Figure 9 reveals that as rank increases there is a decrease in the surface area of chars. Increasing heat treatment temperature further reduces char surface area. These results reflect the increases in average pore size as heat treatment increases.

The volume fraction of pores will be estimated from 'absolute intensity' data when the primary calibrated sample is received. At that stage, we will be in a position to fully evaluate the SAXS procedure for characterizing the pore structures of coal chars.

EFFECT OF CARBON DEPOSITION ON THE POROSITY AND REACTIVITY OF CHARS

Introduction

For the production of low and high BTU gases by coal gasification, it is desirable to maximize gasification rates. The major factors which control the reactivity of carbonaceous solids to oxygen, carbon dioxide, water, and hydrogen are[1, 13] : (i) concentration of active carbon sites located at the edges of layer planes, (ii) presence of catalytic inorganic impurities, and (iii) diffusional

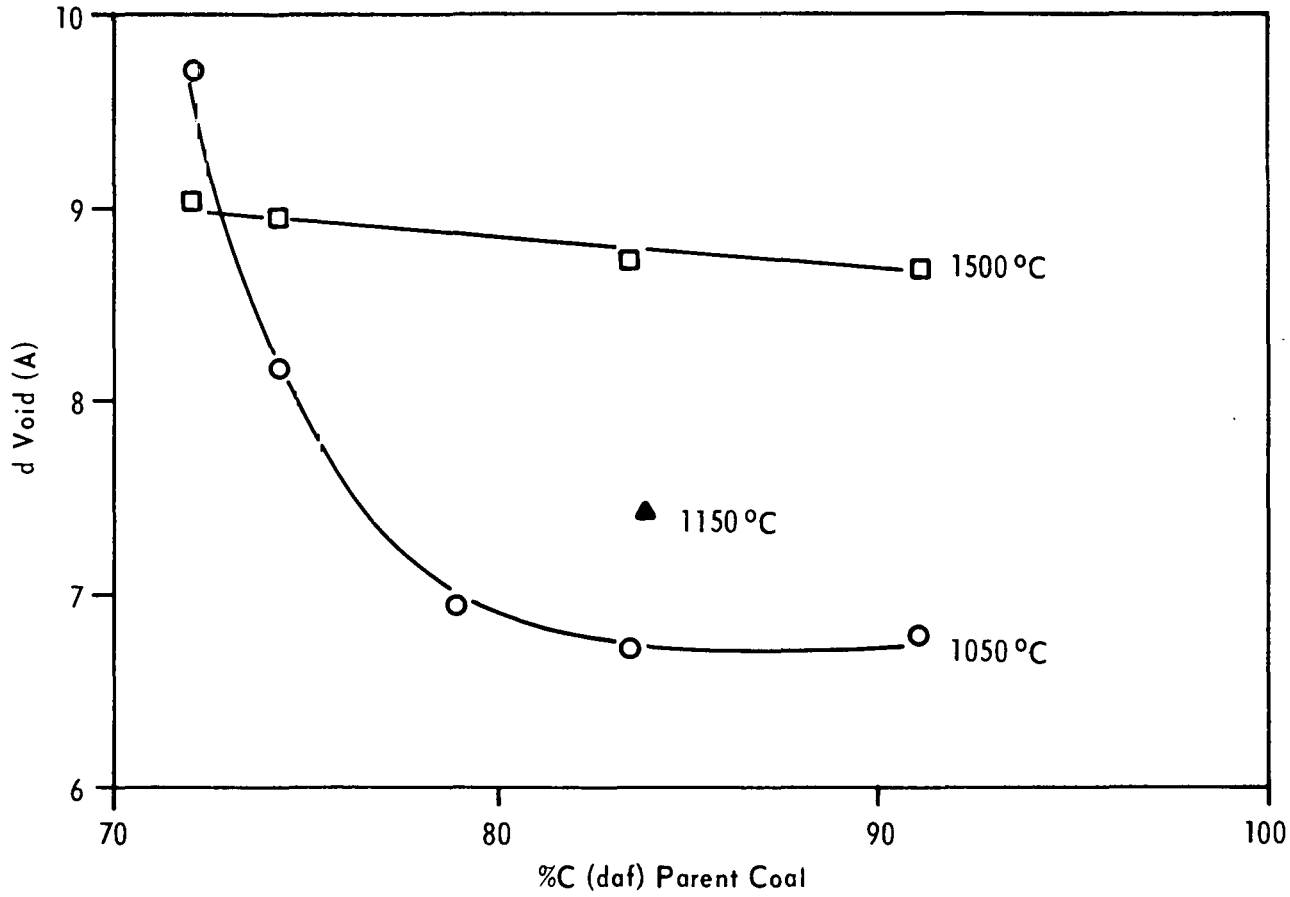

Figure 7. VARIATION OF D VOIDS WITH RANK OF PARENT COAL

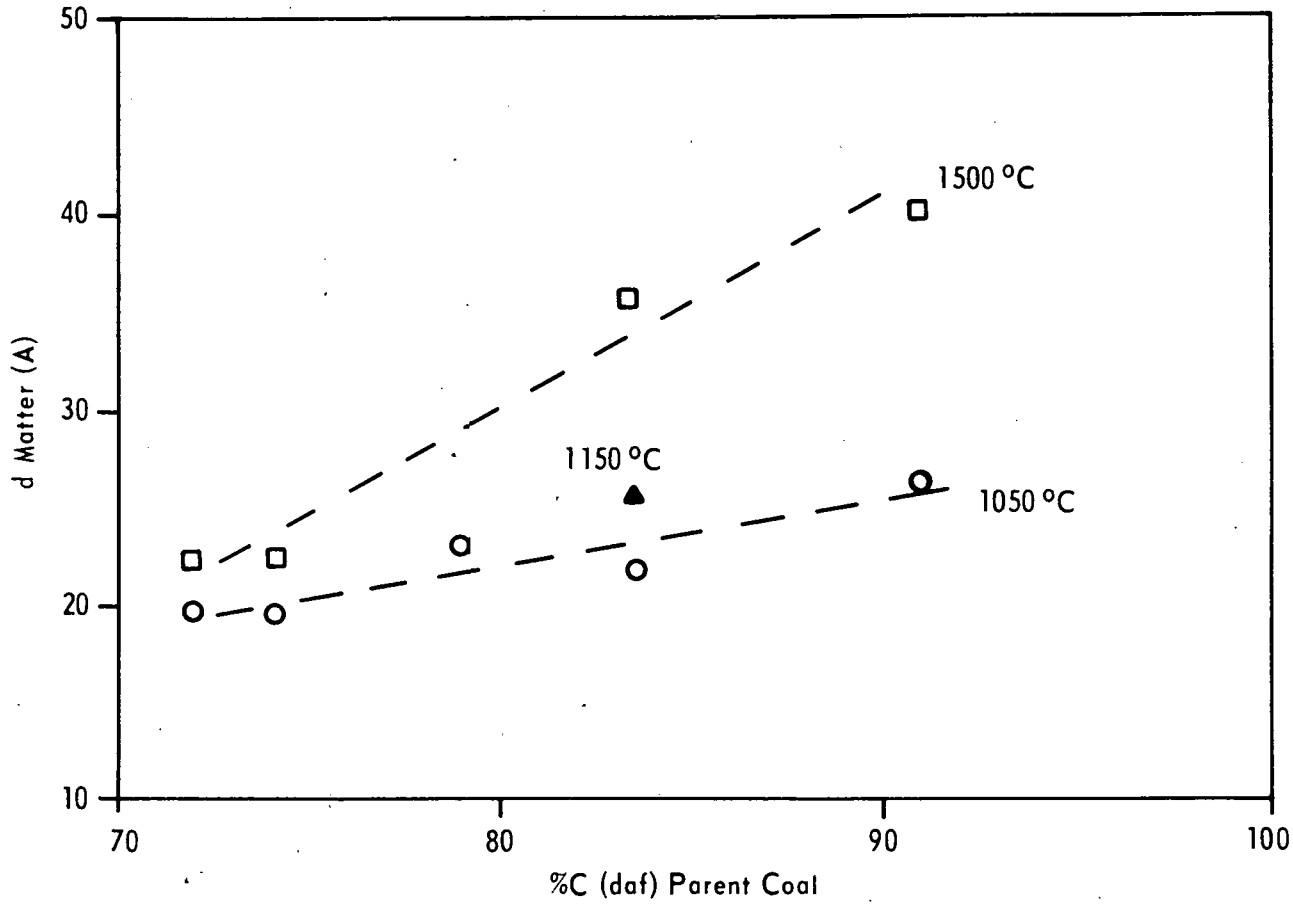

Figure 8. VARIATION OF D MATTER WITH RANK OF PARENT COAL

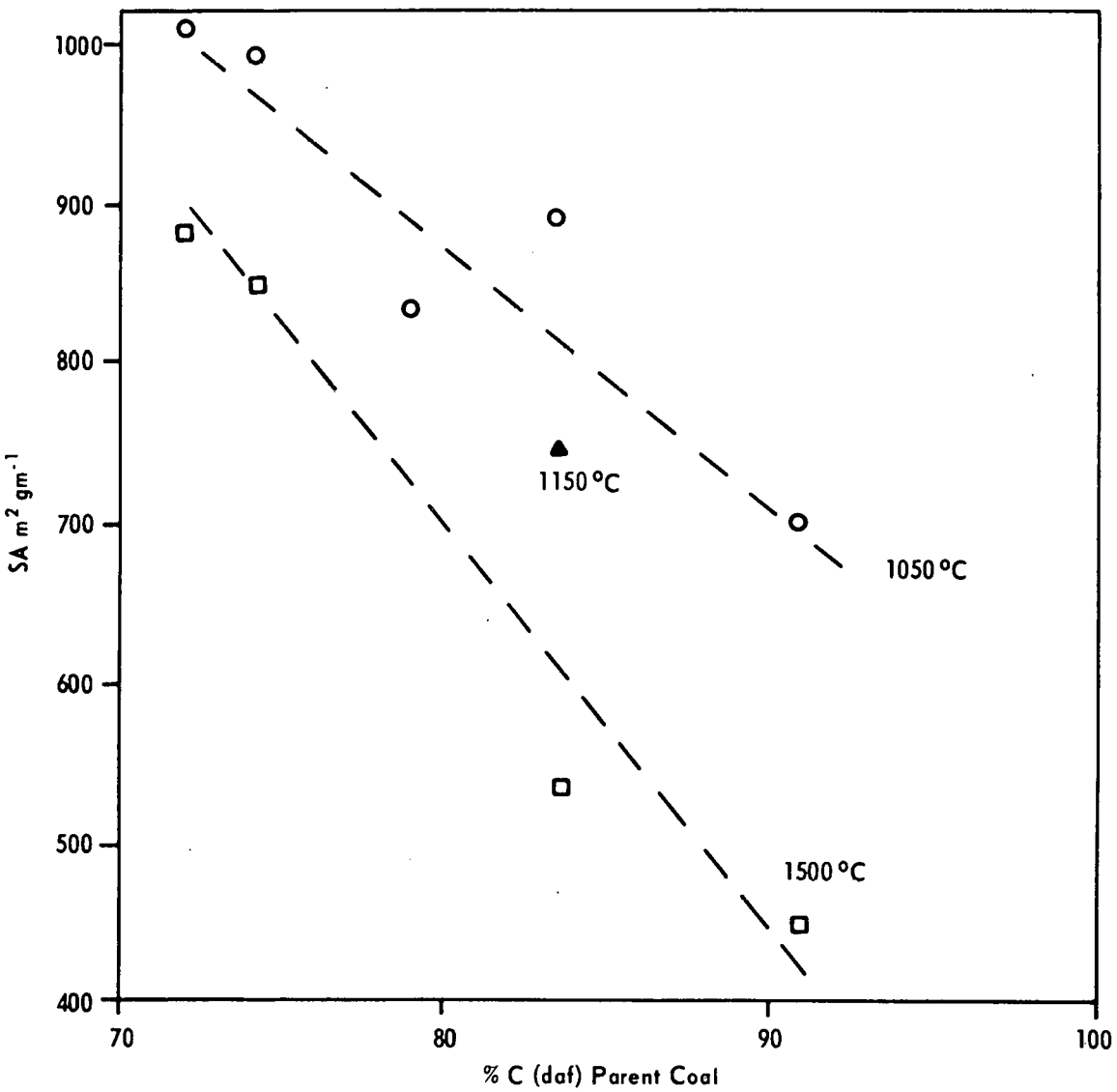

Figure 9. VARIATION OF SURFACE AREA WITH RANK OF PARENT COAL

limitations on how rapidly the reactant gas molecules can reach the active sites. Since devolatilization (pyrolysis) precedes the gasification step, it is probable that methane (released as a constituent of volatile matter) while diffusing out of the micropore structure into the main gas stream may crack on the carbon surface depositing carbon. The phenomenon of chemical vapor deposition resulting from the cracking of methane on various surfaces has been widely reported in the literature[14,15]. Carbon deposition or carbon deposited on the char surface may adversely affect the three factors, referred to above, controlling the char reactivity. To the best of our knowledge the effect of carbon deposition on a char surface on the aforementioned factors has not previously been studied. The aim of the present study is to investigate the effect of carbon deposition within the pore volume of chars on changes in the porosity, the rate at which reactant molecules can diffuse into (or product molecules can diffuse out of) the internal pore structure and subsequent reactivity of the chars during gasification.

Experimental

A North Dakota lignite coal (PSOC-87) was selected for the present study. Proximate and ultimate analyses of the coal are given in Table 3.

Table 3. Proximate and Ultimate Analysis of Raw Coal

Content	Weight %
Proximate Analysis	
Ash (dry)	11.5
Volatile matter (daf)	54.2
Fixed carbon (daf)	45.8
Ultimate Analysis (daf)	
C	71.2
H	5.3
N	0.56
S	0.46
O (by difference)	22.5

A commercial activated carbon (BPL, 12 x 30, supplied by Calgon Corporation, Pittsburgh) was also used in a few studies. This carbon is reported to have a mercury density of 0.85 g/cm^3, a helium density of 2.1 g/cm^3 and an open pore volume of 0.70 cm^3/g.

About 30 g of raw coal (40 x 100 mesh) were taken in a graphite boat. The boat was placed in a tube furnace. Prepurified nitrogen was flushed through the tube furnace for 1 hr. Following this, the coal was heated to 855°C at a rate of 10°C/min. Soak time at 855°C was 2 hr. The char was subsequently cooled in nitrogen to room temperature. The char has a mercury density of 1.32 g/cm^3, a helium density of 2.05 g/cm^3, an open pore volume of 0.27 cm^3/g and an open porosity of 35.6 percent.

In order to study the effect of inorganic impurities associated with the char on carbon deposited, the char, prior to carbon deposition, was treated with 10 volume percent hydrochloric acid close to its boiling point (about 100°C) for 3 hr. The char was then washed free of chloride ions with hot distilled water. This treatment decreased the ash content of the char, on a dry basis, from 11.5 to 6.6 percent.

For studying the kinetics of carbon deposition on the char and activated carbon, a Fisher TGA unit, Model 422, was used. A mixture of methane and nitrogen at a total pressure of 1 atm and a methane partial pressure of 50 torr was used for carbon deposition. For TGA runs, about 4 mg of char were taken in a platinum pan. After flushing out the whole system with prepurified nitrogen (flow rate 300 cc/min) for 2 hr, heating was started at a rate of 10°C/min. As soon as the desired carbon deposition temperature was attained, it was held constant until the sample weight became constant. At this stage, nitrogen was replaced by the methane-nitrogen mixture at the same flow rate. Weight changes due to carbon deposition were recorded as a function of time.

Amounts of carbon deposited on the 855°C char at 815, 825 and 855°C as a function of time are plotted in Figure 10. In each case the rate of carbon deposition first increases gradually with time to a maximum, then gradually decreases with time until finally the remaining rate falls abruptly to essentially zero. The maximum amount of carbon deposited increases with increasing reaction temperature.

Acid washing of the char decreases the extent, as well as the rate, of carbon deposition (Figure 10). When the amounts of carbon deposited at 815°C on the acid-washed chars are considered, it is evident that the removal of mineral matter by acid treatment decreases the extent of total carbon deposition by about 30 percent. Furthermore, the limiting constant carbon deposition on the acid-washed sample is attained after about 115 min compared to only 50 min for the raw char.

Carbon deposition was next studied on the activated carbon. The results are also plotted in Figure 10. At 815°C maximum carbon deposition on the activated carbon is twice that found on the 855°C lignite char. However, when the rates of carbon deposition are considered on a fractional basis, that is, ratio amount of carbon deposited at a given time to the maximum amount of carbon deposited, the rate is faster in the case of the raw char.

According to the data of Palmer and Cullis[14], the rate of homogeneous cracking of methane at the maximum temperature used in this study (that is, 855°C) would be slow. In this laboratory, Hoffman[16] has recently shown that a carbon surface is a catalyst for the decomposition of propylene to carbon, ethylene and methane and, further, that inorganic impurities in the carbon are still better catalysts. Therefore, it was expected that a significant rate of carbon deposited from methane would be found at 815-855°C over the lignite char and that this rate would be reduced following acid treatment of the char to remove some organic impurities. What was not predictable was the amount of carbon which would be deposited on the char. As seen in Figure 10, carbon deposition stops abruptly on both the raw and acid-washed chars, with the

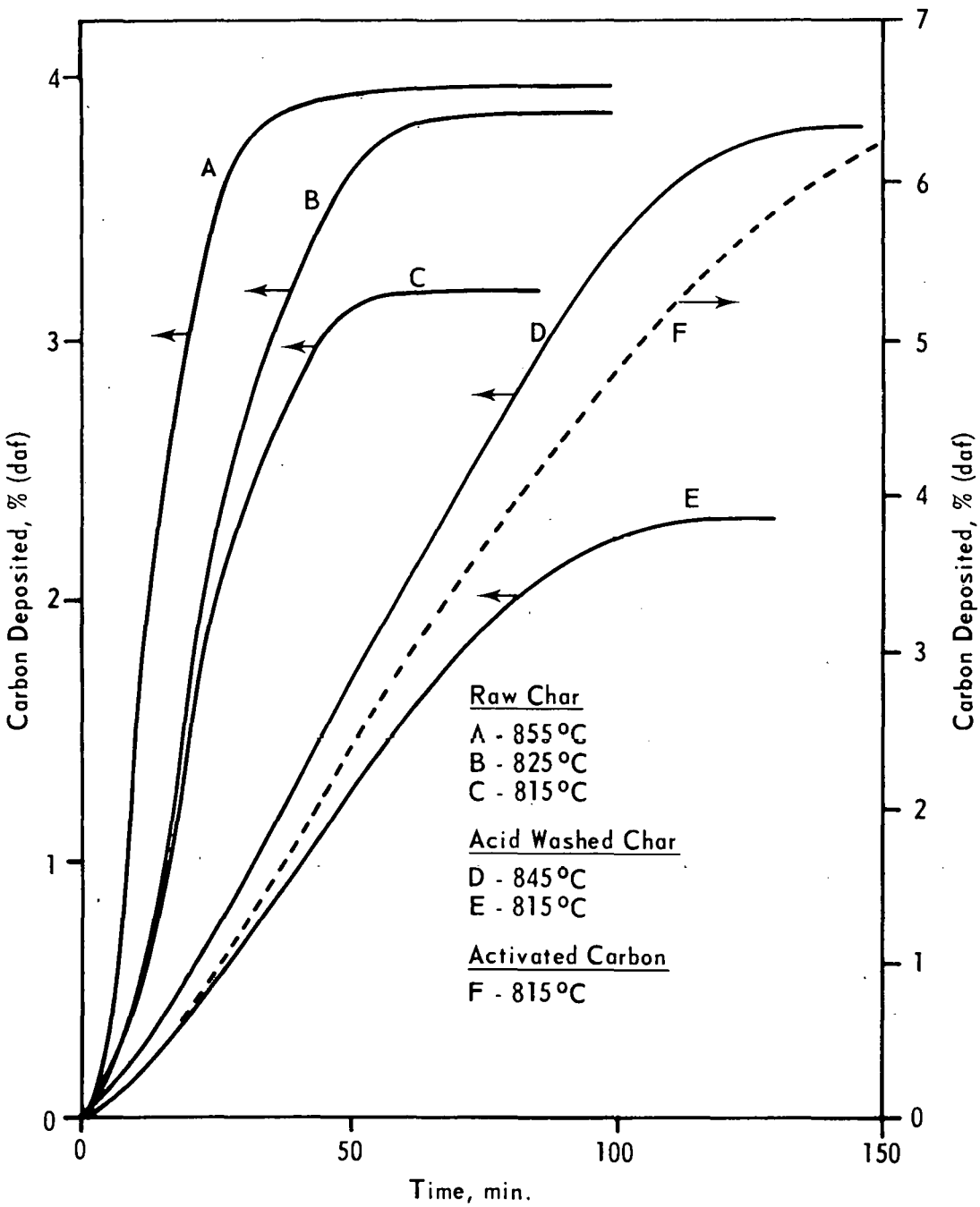

Figure 10. CARBON DEPOSITION ON THE 850°C CHAR AND ACTIVATED CARBON

total amount deposited on the acid-washed char being less than that on the raw char. Assuming that the density of the deposited carbon is essentially the same as that of the carbon in the raw lignite char, the maximum amount of carbon deposited is substantially less than that which could be accommodated within the open pore volume of the char. That is, the raw char had an open porosity of 35.6 percent but maximum carbon deposited at 855°C was only about 4 percent (Figure 10).

There are at least two explanations for these results. First, the inorganic impurities are the active sites for methane cracking and when they are covered, significant methane decomposition stops. Second, the apertures in the lignite char are closed sufficiently by carbon deposition so that methane no longer has access into the microporosity within the char.

The effect of carbon deposition within the pore volume of the lignite char on changes in the porosity and subsequent reactivity of the char during gasification will be studied.

REACTIVITIES OF AMERICAN COAL CHARS IN STEAM

Introduction

The objectives of the present work were outlined in the previous ERDA progress reports. The aim of this report is to study the effect of mineral matter removal from coals and chars on subsequent reactivity in steam. The effect of particle size of char and hydrogen addition to steam on reactivity has also been investigated. For the most reactive char (PSOC-91), effect of flow rate and partial pressure of water vapor on reactivity in steam as well as a steam-hydrogen mixture has also been studied.

Experimental

Mineral matter removal was affected by treating either the coals, prior to carbonization, or raw chars with 10 volume percent hydrochloric acid or a 1:1 hydrochloric-hydrofluoric acid mixture.

Reactivities of the acid washed chars, their surface areas (measured by nitrogen and carbon dioxide adsorption) and their ash contents (estimated by heating the chars in air to 600°C) are given in Table 4. Figure 11 shows graphically how the removal of mineral matter affects reactivity profiles of chars. Reactivities of the chars derived from acid washed coals, with the exception of LV bituminous and anthracite chars (PSOC-127 and 81), decrease significantly upon mineral matter removal (Table 4). Removal of mineral matter from coals prior to their carbonization brings about profound changes in surface area. The decrease in char reactivity and changes in surface area are less pronounced when the raw chars rather than the coal precursors are acid-washed.

In the case of the raw lignite char, reactivity is essentially independent of particle size in the range 40 x 100 to 200 x 325 mesh. On the other hand, in

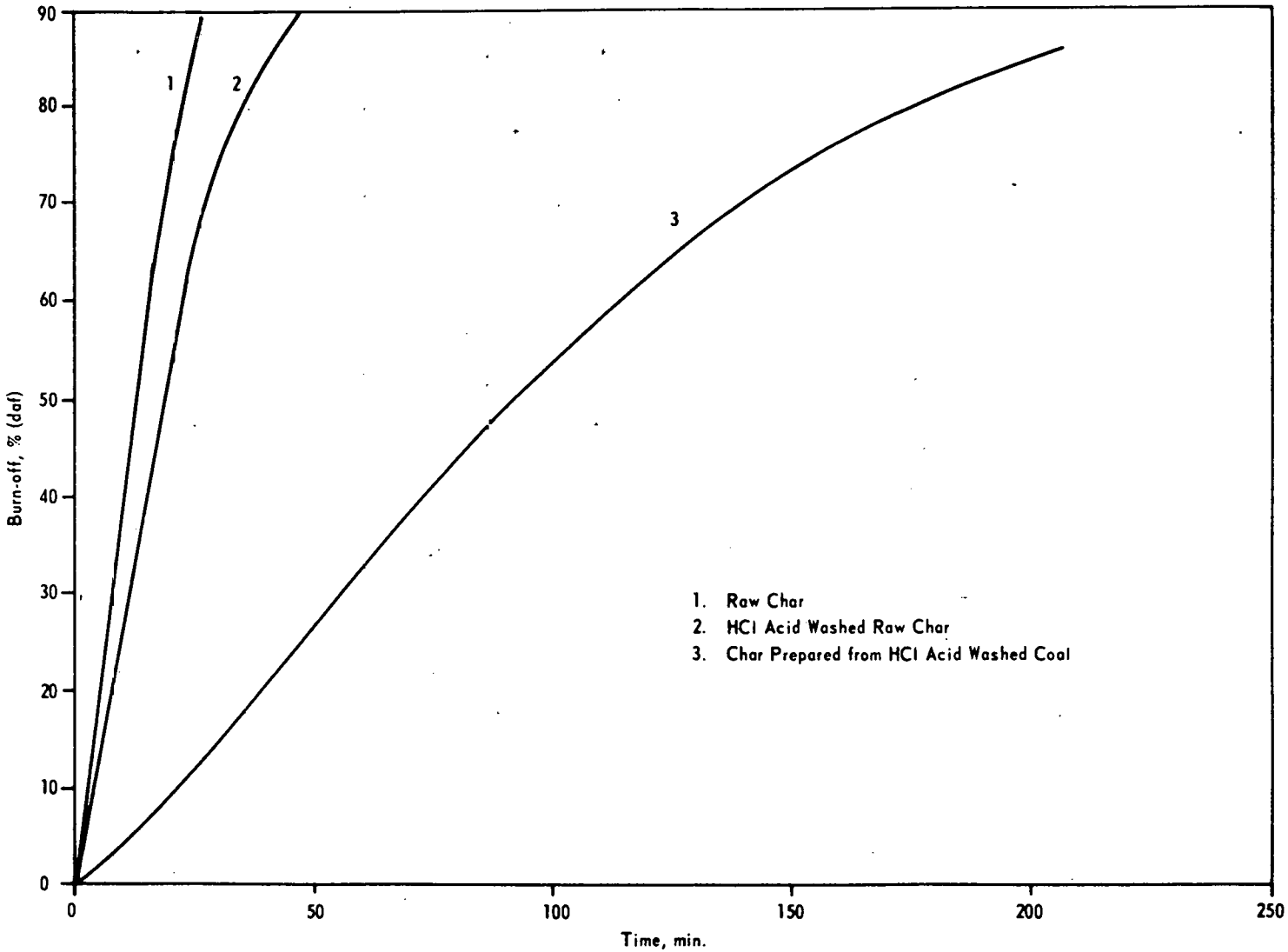

Figure 11. BURN-OFF CURVES IN STEAM AT 910 °C FOR PSOC-101 CHARS

Table 4. Influence of Mineral Matter Removal on

Reactivity and Surface Area of Chars

PSOC Char No.	Surface Area (m^2g^{-1}) Nitrogen	Carbon Dioxide	Ash % dry	Reactivity mg hr^{-1} mg^{-1}
91	31	420	10.9	2.88
91 AW-Char*	17	470	7.2	1.75
91 AW-Coal**	88	912	1.3	0.43
87	93	260	13.1	2.81
87 AW-Char	106	500	6.0	1.08
87 AW-Coal	11	610	2.6	0.33
87 Dem-Coal***	1	600	0.0	0.38
138	120	560	16.0	1.17
138 AW-Char	11	497	11.6	0.88
138 AW-Coal	4	680	9.6	0.34
138 Dem-Coal	47	115	0.9	0.19
101	62	400	8.2	2.46
101 AW-Char	17	359	5.4	1.57
101 AW-Coal	3	670	1.1	0.35
127	2	12	6.7	0.011
127 Dem-Coal	4	37	0.0	0.14
81	1	39	6.4	0.13
81 AW-Char	<1	47	6.1	0.14
81 AW-Coal	<1	40	5.8	0.14
81 Dem-Coal	<1	56	0.9	0.19

* Raw char HCl acid-washed
** Char prepared from HCl acid-washed coal precursor
*** Char prepared from HCl-HF acid-washed coal precursor

the case of the PSOC-127 char, reactivity increases about four-fold upon particle size reduction from 40 x 100 to 200 x 325 mesh, indicating that the reaction in this case is partly diffusion-controlled. Upon demineralization, reactivity of PSOC-87 char for each size fraction decreases sharply. Reactivity of the demineralized char increases monotonically with decrease in particle size. Reactivity of the PSOC-127 char, for each particle size, is seen to increase appreciably upon mineral matter removal. It was previously suggested that since acid washing markedly lowers inorganic impurity content, where these impurities would be expected to be primarily large discrete mineral matter particles in this coal, macro and transitional porosity would be introduced. This, in turn, would sharply lower diffusional resistance to gasification in this char, and thereby, increase reaction rate (Table 5).

Table 5. Effect of Particle Size on Reactivity of Chars

Particle Size Mesh	Reactivity, R_o (mg hr^{-1} mg^{-1})			
	PSOC-87 Char		PSOC-127 Char	
	Raw	Dem	Raw	Dem
40 x 100	2.81	0.38	0.011	0.14
100 x 150	2.61	0.46	0.013	0.22
200 x 325	2.82	0.51	0.043	0.33

In order to study the effect of hydrogen addition to steam on char reactivity, a mixture of nitrogen and hydrogen containing 20 percent hydrogen was bubbled through water at 20°C; the partial pressure of water vapor in the mixture was 17.5 torr. Reactivity profiles for a few selected chars are shown in Figure 12. Reactivity parameters for the various samples studied are given in Table 6. Reactivities of two lignite chars, PSOC-91 and 87, decrease sharply in the presence of hydrogen indicating a strong inhibitive effect of hydrogen. Addition of hydrogen has little or no effect on the reactivities of chars derived from PSOC-26, 22, and 24 coals. Reactivity of the LV bituminous char, PSOC-127, increases by ten-fold in the presence of hydrogen. The addition of hydrogen to steam increases slightly the reactivity of the raw lignite char, PSOC-138, but has an inhibiting effect in the case of the acid washed char. These results suggest that in the case of the PSOC-127 and 138 chars, hydrogen reacts with some catalytically inert inorganic impurity initially present in the char converting it to a catalytically active chemical form and that the inhibitive effect on char reactivity due to hydrogen is more than offset by the catalytic effect of the "regenerated" impurity.

The apparent order of reaction with respect to partial pressure of steam for PSOC-91 char for reaction with steam and steam-hydrogen mixture was determined by varying the partial pressure of water vapor from 6.5 to 17.5 torr. The apparent order for the reaction with steam is 0.60, whereas for the steam-hydrogen reaction it is 0.93 (Figure 13).

The effect of flow rate (in the range 115 to 530 cc/min) on reactivity in steam as well as in the steam-hydrogen mixture was investigated for PSOC-91 char. In each case, partial pressure of steam was the same, that is, 17.5 torr. The results are given in Table 7. These results show clearly the inhibiting effect of hydrogen on char reactivity. Hydrogen is a product of the carbon-steam reaction. For the reaction in steam alone, an increase in flow rate will result in sweeping away the hydrogen liberated, thus decreasing the extent of retardation of the reaction. In the presence of an excess pressure of added hydrogen, this effect is not expected to be discernible.

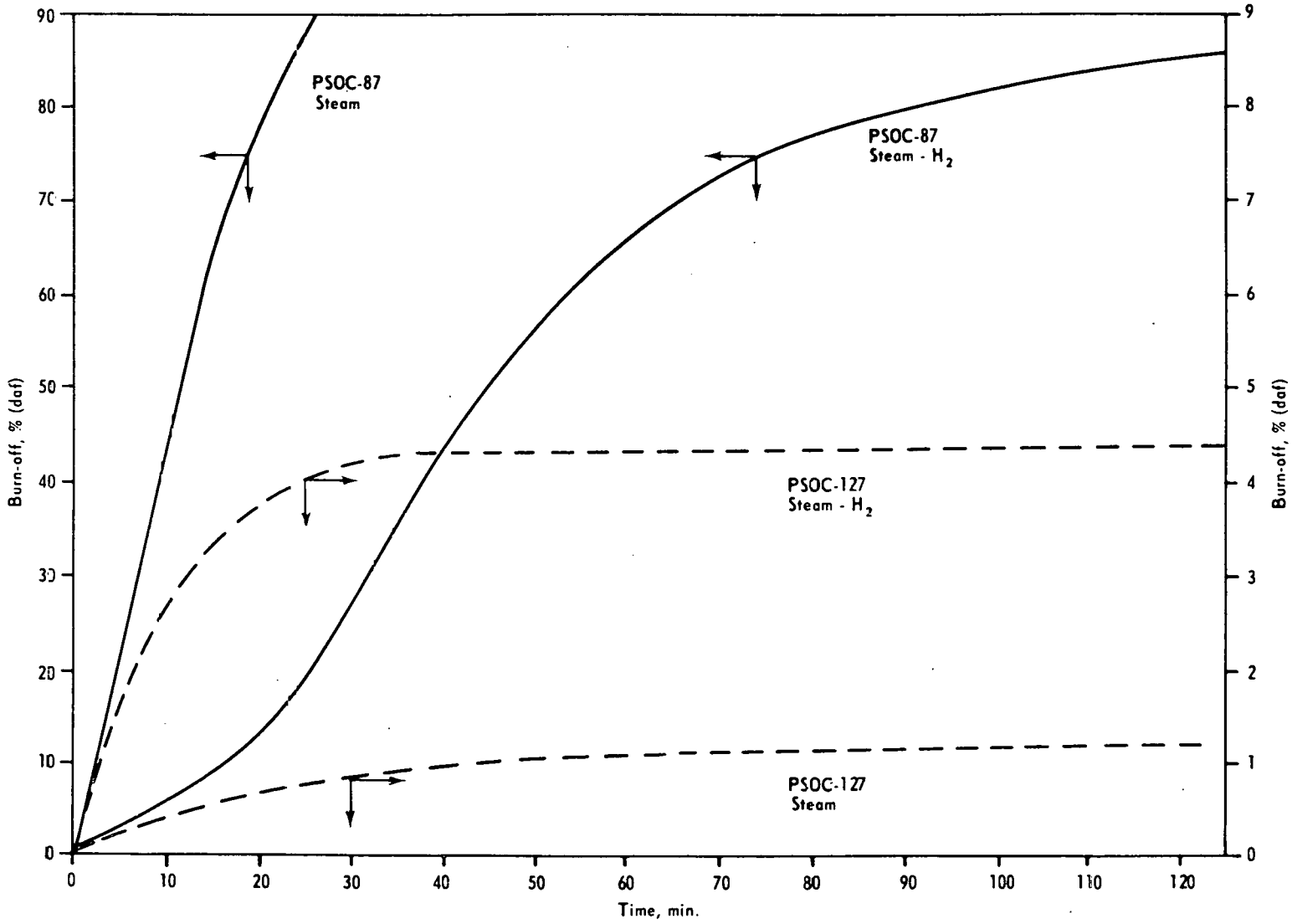

Figure 12. BURN-OFF CURVES FOR PSOC-87 AND 127 CHARS IN STEAM AND STEAM - H_2 MIXTURE AT 910°C

Table 6. Effect of Hydrogen Added to Steam on Reactivity

Parent Coal PSOC No.	Reactivity, R_O, mg hr^{-1} mg^{-1}	
	Steam	Steam-Hydrogen
91	2.88	0.63
91 AW-Char	1.75	0.51
87	2.81	1.02
138	1.17	1.31
138 AW-Char	0.88	0.63
26	0.25	0.24
22	0.45	0.40
24	0.52	0.59
127	0.011	0.20

Table 7. Influence of Partial Pressure of Water Vapor and Flow Rate on Reactivity of PSOC-91 Char

Partial Pressure (torr)	Reactivity, R_O, (mg hr^{-1} mg^{-1})	
	Steam	Steam-Hydrogen
6.5	1.62	0.26
9.2	1.93	0.36
17.5	2.88	0.63
Flow Rate (cc/min)		
111	2.65	0.63
350	2.88	0.64
530	3.20	0.63

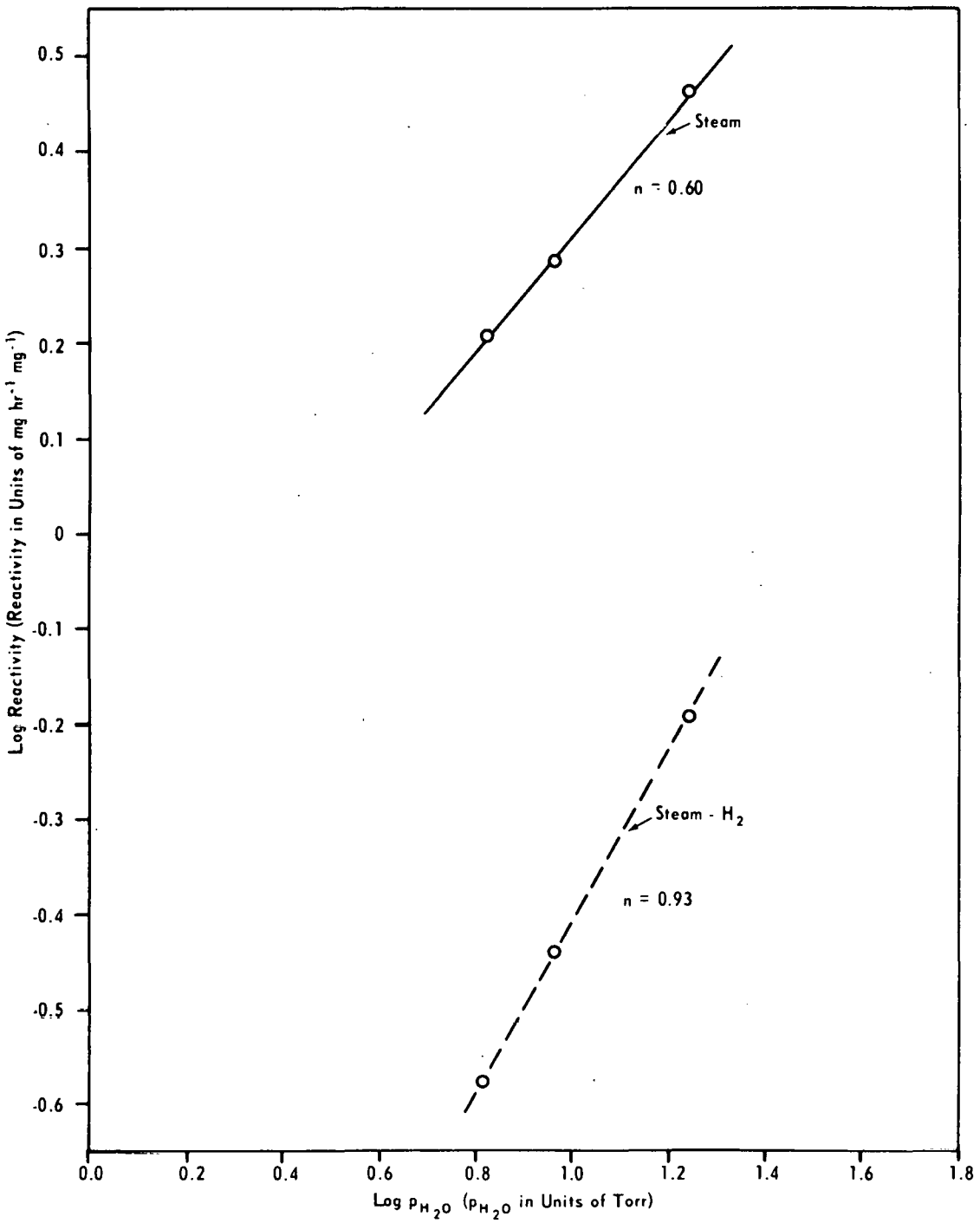

Figure 13. INFLUENCE OF WATER VAPOR PARTIAL PRESSURE ON THE REACTIVITY OF PSOC-91 CHAR IN STEAM AND STEAM - H_2 MIXTURE AT 910°C

REACTIVITY OF ION EXCHANGED LIGNITE CHARS TO STEAM

Introduction

Reactivities of chars prepared from 28 x 48 mesh size fractions of raw demineralized, and cation exchanged Texas lignite were measured in a fluidized bed of steam at reaction temperatures of 650°C, 700°C, 735°C, and 750°C. Variables studied in this part of the investigation were heat treatment temperature (700, 800, and 900°C), amount of Ca^{++} exchanged (1-13% by weight), end pH of exchange (7.5, 9.5, and 11.0), type of cation exchanged (K^+, Na^+, Ca^+, Mg^{++}, and Fe^{+++}), anion solution in which exchange was performed (acetate and nitrate), and level of mineral matter (raw and demineralized). Additionally, two raw coal chars (800°C and 900°C) were demineralized, oxidized by treatment with nitric acid and ion exchanged. Reactivities of these chars were measured under the same conditions mentioned above. Variables studied in this part of the investigation were reheat temperature (650°C, 700°C, 750°C, 800°C, and 850°C) and type of cation exchanged (Na^+, Ca^{++}, Mg^{++}, and Fe^{+++}). Ash content, ash composition, moisture content, mercury and helium densities, size distribution, and surface area have been determined for all samples.

Experimental

Demineralized coal was ion exchanged in K^+ and Mg^{++} acetate solution. The exchanged coals were charred to 800°C and reacted at 650°C. The 800°C nitric acid treated char was exchanged in Fe^{+++}, Mg^{++}, and Na^+ solutions. The exchanged chars were reheated to 800°C and reacted at 650°C. All samples were characterized by previously stated methods. Determination of Ca^{++} in the raw coal sample which could be removed by acid washing was made.

A plot of burn-off as a function of time for 800°C chars prepared from coals exchanged with various cations to a level of 0.3 millimoles per gram of dry, ash-free coal was discussed in the previous report. In addition, the char prepared from the K^+ exchanged coal has been reacted. The char containing the potassium is more reactive than any of the other chars (Table 8).

Burn-off curves of 800°C chars prepared from coals exchanged in magnesium acetate and nitrate solutions (0.3 millimoles/g coal (daf)) are identical indicating that the nitrate and acetate anions have a similar effect on charring and reactivity.

Burn-off curves of 800°C chars which were demineralized, treated with nitric acid, and exchanged with various cations prior to reheating to 800°C and reacted at 650°C, are reproduced in Figure 14. The Na^+ char yields a straight line. The curves for the chars containing Fe^{+++} and Ca^{++} cross over the curve for the Na^+ containing char. Extrapolation of the curves for the Fe^{+++} and Ca^{++} chars cross over at approximately 20 percent burn-off. Again, the magnesium char is much less reactive. Reactives of the 800°C, demineralized, nitric acid treated cation exchanged chars are listed in Table 9.

Work for the next quarter will center around consolidation of data and x-ray diffraction to study crystallographic structure.

Table 8. Reactivities in Steam at 650°C of Chars

Prepared from Various Cation-Exchanged Coals

Cation	Loading of Cation (millimoles/g of coal)	Reactivity, 10% Burn-off (g/g hr) (daf)
K	0.3	0.18
Na	0.3	0.13
Fe	0.3	0.12
Ca	0.3	0.11
Mg	0.3	0.03

Table 9. Steam Reactivities at 650°C of

800°C Cation-Exchanged Chars

Ion Exchanged	Millimoles of Ion Exchanged/ g of Coal	Reactivity, 10% Burn-off (g/g hr) (daf)
Na	0.2	0.11
Fe	0.2	0.11
Ca	0.2	0.09
Mg	0.2	0.03

As previously reported, large amounts of inorganic elements can be added to raw lignites or lignite chars using ion exchange. Such exchange results in large increases in reactivity of the char to steam. A linear relationship between reactivity and Ca^{++} loading in the char indicates a constant effective utilization of the catalyst in 1 to 13 percent loading range. The 13 percent loading has been the most extreme case studied to date. Reactivity was over 100 times greater than that of the char prepared from the demineralized coal. Reheating of the 900°C raw coal char which had been demineralized, nitric acid treated, and Ca^{++} exchanged resulted in two discrete reactivity decreases occurring between reheat temperatures of 650°C and 700°C, and 800°C and 850°C. The results indicate a complex relationship between pore structure, catalyst behavior, and reactivity. The reactivity of the char prepared from the Fe^{+++} exchanged coal decreases rapidly with burn-off. Above 12.5 percent burn-off the order of activity of the catalysts is Na>Ca>Fe = Mg. No effect of end point pH of exchange on reactivity could be determined.

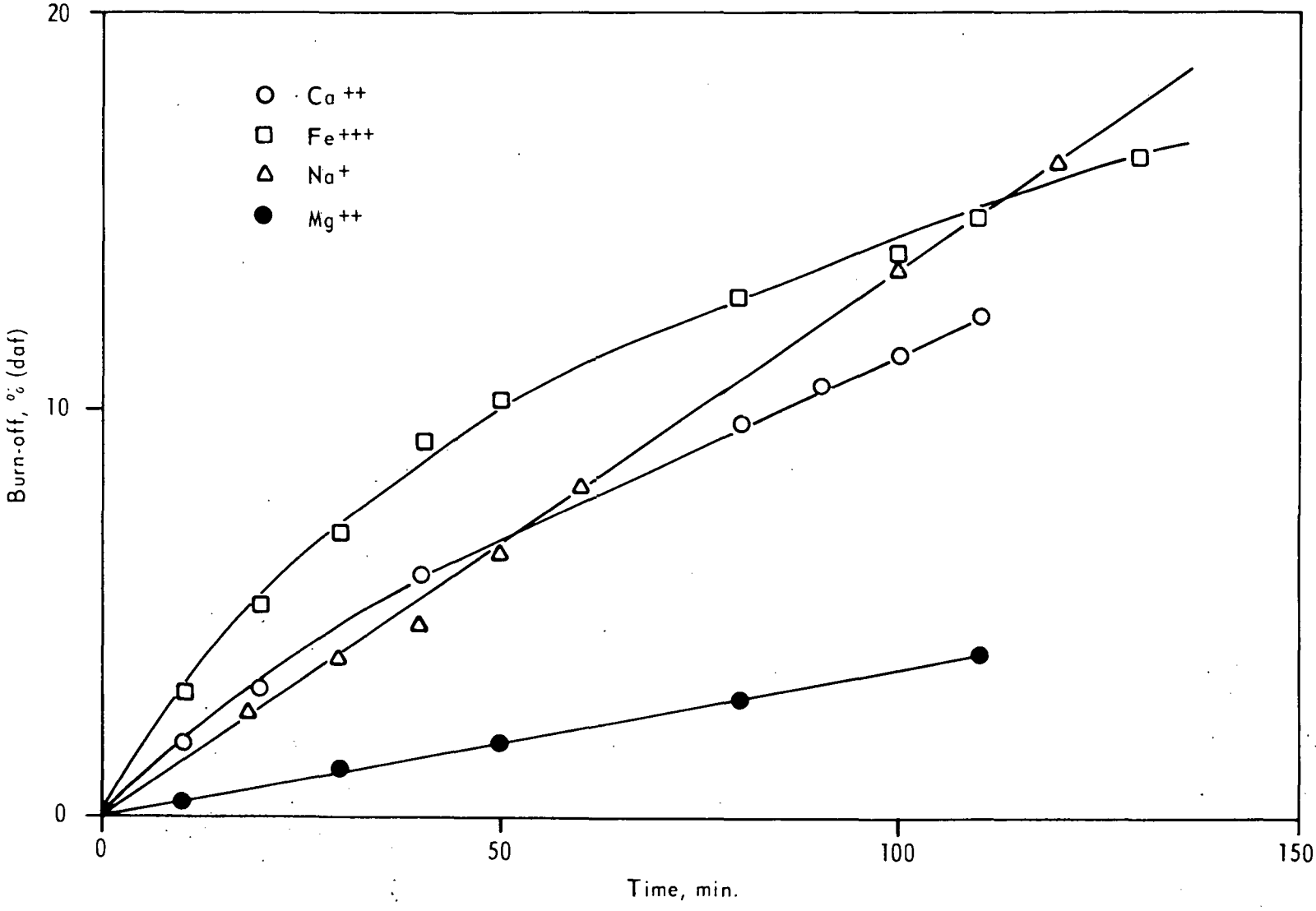

Figure 14. BURN-OFF CURVES OF VARIOUS EXCHANGED CHARS PREPARED FROM 800°C DEMINERALIZED NITRIC ACID TREATED CHARS

In addition to previously stated results, the following conclusions can be added. K^+ containing char is more reactive than any of the other exchanged chars. The nitrate and acetate anion have the same effect on charring and subsequent reactivity. Reactivity of thermally stable char is greater than predicted from reactivity of chars prepared from various exchanged coals.

FACET V-A: COMBUSTION OF CHARS AND LOW VOLATILE FUELS

COMBUSTION OF CHAR AND ANTHRACITE COAL IN LARGE UTILITY BOILERS

Introduction

Work has continued focusing on the development of computer models to analyze and explain past experiments and to design future ones. A model of a pulverized char flame with an infinite parallel plane geometry was presented in the previous quarterly report.

Now the study of the infinite parallel plane model has provided insight into the effects of two major variables: fuel reactivity and combustor length.

Experimental

The first effect to be investigated in this recent infinite parallel plane computer model study was that of fuel reactivity. The standard reactivity used in this study is that given by Field[17] for a low rank char. The other reactivities used in the study were fractional multiples of this standard value, with β, the fractional multiplier, being defined as the current reactivity divided by the Field standard reactivity at the same temperature.

The general effect of fuel reactivity on combustor temperature profile can easily be seen in Figure 15. There, combustor temperature profiles from inlet to outlet (left to right) are plotted for one fuel of standard reactivity and one of reactivity 0.15 times the standard one, for a combustor length of 120 cm. Qualitatively speaking, the effect of changing to lower reactivity is to delay the initial temperature rise and to flatten out the region of highest temperature. These types of qualitative differences have been noted in our previously published experimental work[18] involving the Exxon Illinois and Wyodak chars and the lower reactivity FMC COED char. Some attempt at a more quantitative comparison will now be made.

Tables 10 and 11 show the effect of fuel reactivity on various calculated parameters for combustor lengths of 90 and 120 cm respectively, where the following definitions hold: β is the fractional reactivity multiplier described above; T_{max} is the maximum combustor temperature; X_{max} is the distance from the cold inlet wall where T_{max} occurs; $X_{74\%}$ is the distance from the cold inlet wall where 74 percent of the fuel has been consumed (75% represents "complete" combustion due to the -25% excess air condition used); T_{final} is the combustor exit temperature; and T_{w2} is the exit (hot) wall temperature.

In these two tables, one can follow the continuous increases of X_{max}, $X_{74\%}$, T_{final}, and T_{w2}, and the continuous decrease of T_{max} with decreasing fuel reactivity. In Figure 16, T_{max} and T_{final} are plotted as solid lines versus β

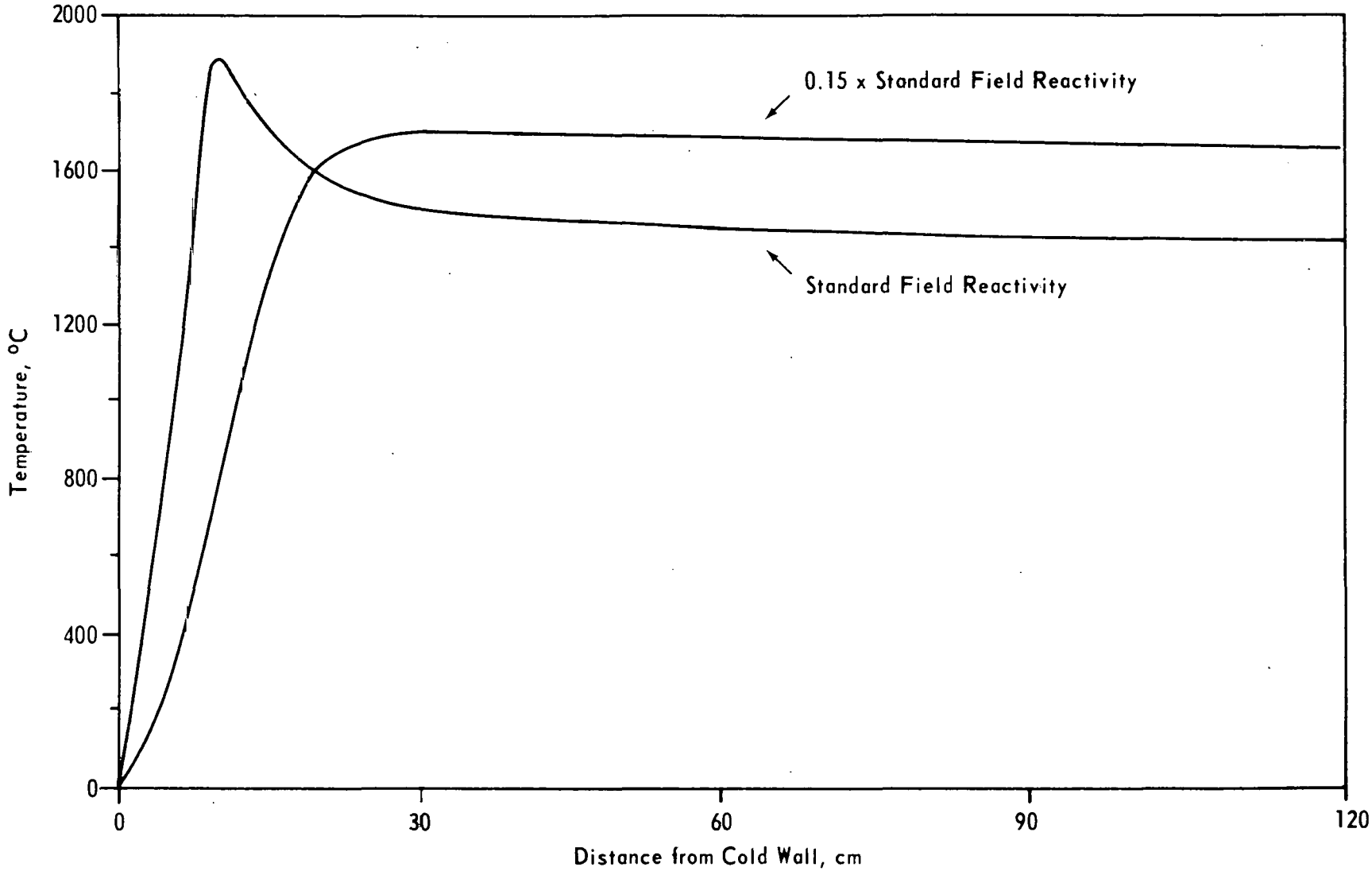

Figure 15. INFLUENCE OF REACTIVITY ON COMBUSTOR TEMPERATURE PROFILE.

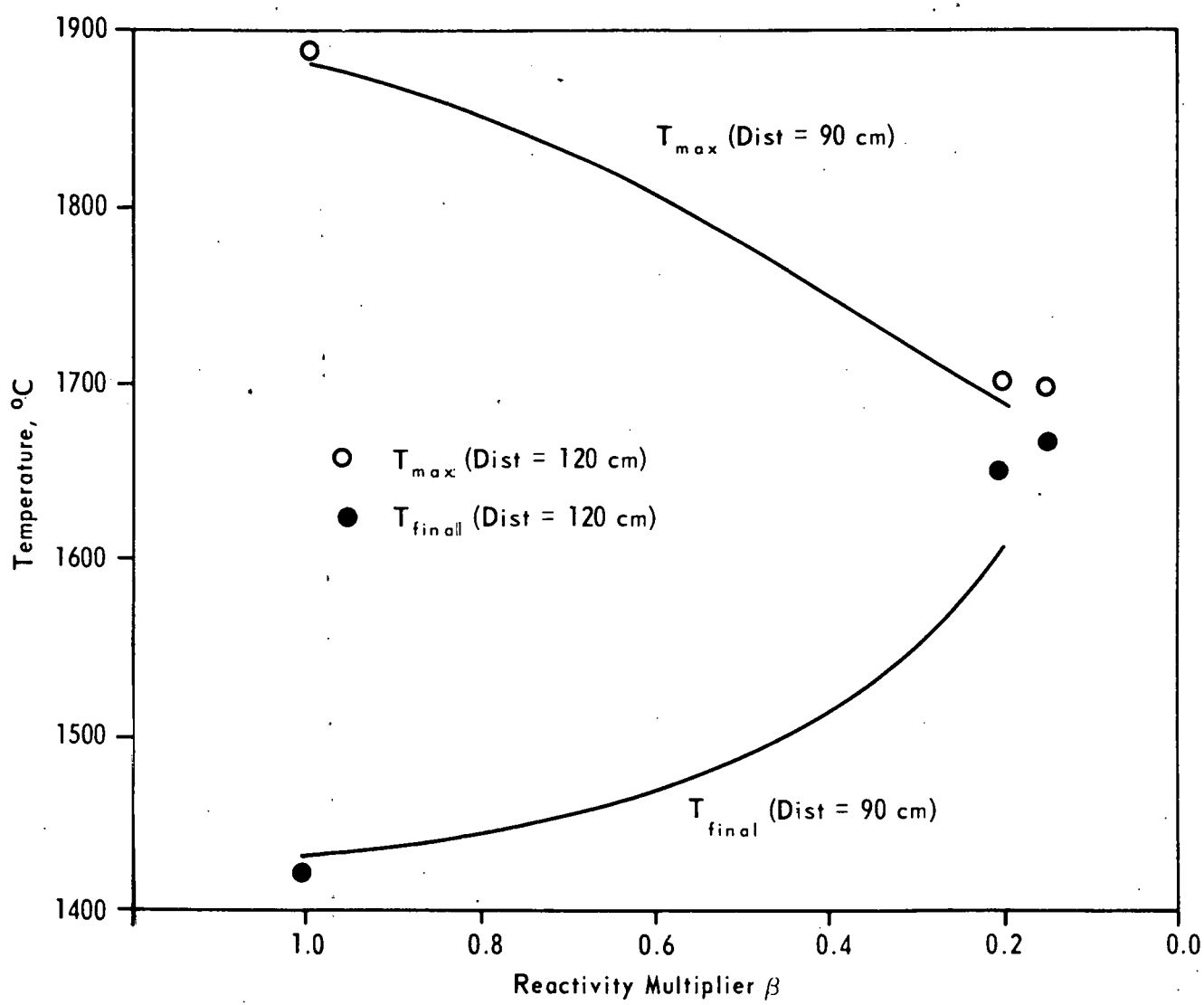

Figure 16. INFLUENCE OF REACTIVITY ON T_{max} AND T_{final}

Table 10. Effect of Fuel Reactivity on Calculated Parameters (Distance = 90 cm)

β	T_{max}(C)	X_{max}(cm)	$X_{74\%}$(cm)	T_{final}(C)	T_{w2}(C)
1.00	1884	9.72	23.16	1428	1414
0.75	1843	10.74	28.56	1450	1437
0.60	1810	11.52	33.00	1471	1458
0.45	1770	13.02	41.10	1501	1489
0.30	1721	16.38	58.80	1553	1540
0.20	1693	23.16	82.20	1610	1596

Table 11. Effect of Fuel Reactivity on Calculated Parameters (Distance = 120 cm)

β	T_{max}(C)	X_{max}(cm)	$X_{74\%}$(cm)	T_{final}(C)	T_{w2}(C)
1.00	1886	9.66	23.10	1421	1408
0.20	1705	21.24	81.10	1653	1655
0.15	1702	32.94	102.00	1671	1664

(fuel reactivity multiplier) for a combustor length of 90 cm and as single points for a combustor length of 120 cm. Only three computer runs were made at the greater combustor length of 120 cm due to the increased complexity and cost of obtaining solutions at this length.

The plot depicts the continuous rise of T_{final} and the continuous decline of T_{max} with decreasing fuel reactivity (lower β values). Logically speaking, T_{final} can never exceed T_{max}, since T_{max} by definition is the maximum combustor temperature obtained. The single points representing the calculations done for the 120 cm combustor show that for the lowest reactivities run (β = 0.15 and β = 0.20), the T_{final} points appear to be assymptotically approaching the T_{max} points. For both combustor lengths plotted, the difference between T_{max} and T_{final} is approximately 600°C for the standard reactivity calculations and declines to about 30°C for the lowest reactivity used (β = 0.15). Thus, the difference between T_{max} and T_{final} is substantially different for high and low reactivity fuels.

The distance from the cold inlet wall to the location of T_{max} also varies appreciably. In Table 11, a factor of 3.4 variation is seen in the X_{max} distance in going from β = 1.00 to β = 0.15 for the 120 cm combustor. It should be

emphasized that fuel reactivity alone is responsible for this shift. $X_{74\%}$ also shows similar behavior with reactivity variations. And finally, it can be seen from the tables that at the lowest reactivities used, the hot temperature (T_{w2}), like T_{final}, approaches the T_{max} value.

Therefore, very dramatic but systematic change in qualitative and quantitative combustor behavior is attributable to fuel reactivity changes.

The second variable that was checked is that of combustor length. Tables 12 and 13 show the computed results of combustor length variations for two reactivities (β = 1.00 and β = 0.20).

Table 12. Combustor Length Variations
(β = 1.00)

Dist(cm)	T_{max}(C)	X_{max}(cm)	$X_{74\%}$(cm)	T_{final}(C)	T_{w2}(C)
90	1884	9.72	23.16	1428	1414
120	1886	9.66	22.90	1421	1408
150	1886	9.51	22.74	1420	1407

Table 13. Combustor Length Variations
(β = 0.20)

Dist(cm)	T_{max}(C)	X_{max}(cm)	$X_{74\%}$(cm)	T_{final}(C)	T_{w2}(C)
90	1693	23.16	82.20	1610	1596
120	1705	21.24	81.10	1653	1655

For the higher reactivity (β = 1.00), very little effect is seen at all. The T_{max} value rises and X_{max}, $X_{74\%}$, T_{final} and T_{w2} all fall, with all changes being very small indeed. For the lower reactivity value (β = 0.20), T_{max} rises to a much greater extent with increasing combustor length, X_{max} shows an appreciable decrease, $X_{74\%}$ shows less decrease and, in direct contrast to the higher reactivity fuel, T_{final} and T_{w2} both increase and do so substantially. The behavior is easily understood if one realizes that the longer combustor length for the more reactive fuel means more heat transfer time for the tail gases to cool off, and for the less reactive fuel the extra distance means more radiative insulation of the main combustion zone and more nearly complete combustion. Thus, the effect of added combustor length acts in opposite ways depending on whether

a given fuel is fully combusted (as $\beta = 1.00$) or is near extinction (as $\beta = 0.20$) at the shorter combustor lengths.

The two effects investigated here were fuel reactivity and combustion length. The investigation of fuel reactivity variation was an attempt to explain the flame front shifts observed when firing chars of suspected different reactivities[18]. The combustor length study was undertaken to see whether the fixed length of the experimental test furnace used could have influenced the observed behavior. It appears from the results presented here that reactivity variation can be responsible for major shifts in combustor temperature profiles. Further studies decreasing the lowest value of reactivity used will be conducted shortly, based on the encouraging results obtained so far. The fact that the plane-flame furnace used in the experimental facet of this project is of a fixed finite length does seem to magnify the differences between low and high reactivity fuels. Hopefully, further computer model studies will further serve to explain the experimental behavior seen in the earlier stages of this project.

FACET V-B: COMBUSTION OF COAL-OIL EMULSIONS

COAL-OIL-WATER-AIR COMBUSTION MIXTURES

Introduction

During the past quarter the heat transfer characteristics of oil-coal-water-air emulsions and fuel oil No. 2 were studied using a York-Shipley Manufacturing Co. burner. The coal was fed into an emulsifying apparatus as a coal-oil dispersion.

Experimental

The coal-oil dispersion has been prepared by Systems Research Laboratories of Dayton, Ohio and contains 50 percent by weight of coal of size under 100 microns and about 50 percent fuel oil No. 6 with surfactants. This dispersion was fed to the emulsifier with a positive pressure displacement system. The problems encountered with this system were the breaking of a plastic bag inside the pressurized container and the variability in the amount of coal-oil dispersion injected. A gear pump feeding mechanism, constructed with a feed tank containing the coal-oil dispersion, has been developed to introduce the highly viscous mixture into the emulsifier. One problem encountered with this system was backflow from the emulsifier through the gear pump and into the feed tank, and this was corrected by installing a check valve in the line. Sufficient measurements have not revealed the extent of abrasive effect of the coal mixtures on the gear pump.

The experimental technique used in the course of this study is as follows: (i) preheat the furnace for about six hours at a high heating rate using a gas flame, (ii) when the furnace reaches equilibrium (constant wall temperature distribution) fuel oil No. 2 is used to obtain a heat release of 1.25 million Btu per hr, (iii) an oil-water-coal emulsion is then used to obtain a heat release rate of 1.25 million Btu per hr, (iv) samples of the mixture are taken before it enters the burner to determine the percentage of coal and water in the emulsion, (v) heat transfer measurements are made by measuring the water temperature in the cooling tubes at different levels of excess air, (vi) samples of the flue gas are taken and analyzed.

Some results of these experiments are shown in Figure 17. From this figure it can be seen that the introduction of coal into the oil-water emulsion greatly increases the heat transfer characteristics of the mixture. The coal-oil-water emulsion is seen to produce a higher heat transfer rate than that of fuel oil No. 2. This is probably due to an increase in the emissivity of the flame with the introduction of coal particles (under 106μ in size). An effort is currently being undertaken to measure the flame emissivity.

Another factor that effects the heat emitted from a flame is the flame temperature. In order to determine the adiabatic flame temperatures for the different idealized experimental conditions, a computer program was developed

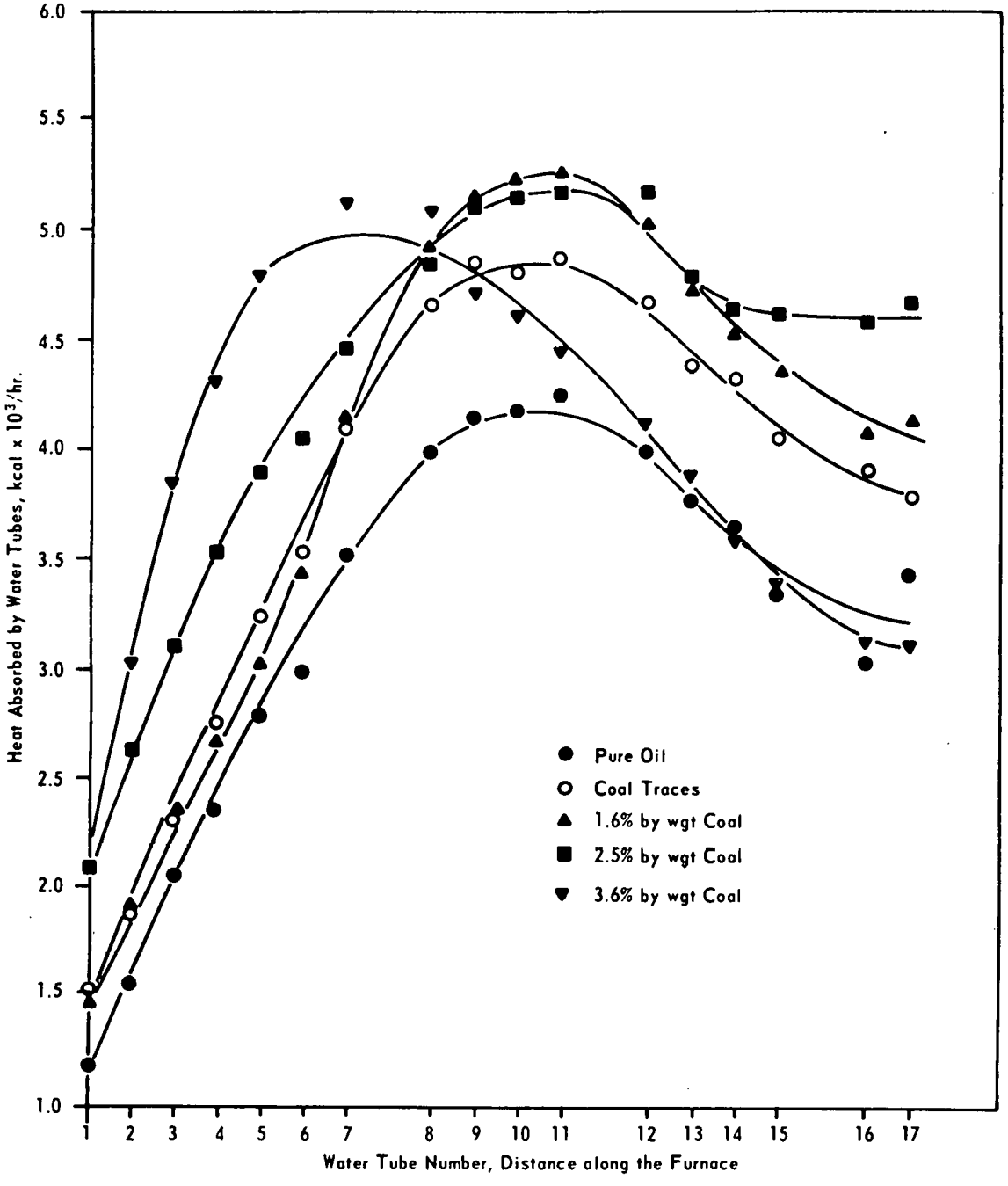

Figure 17. VARIATION OF HEAT FLUX ALONG THE LENGTH OF THE FURNACE AS A FUNCTION OF COAL PERCENTAGE IN THE EMULSION

using the JANAF tables and a basic program from the NASA Lewis Research Center[19]. This program can predict the adiabatic flame temperature at equilibrium, given the chemical composition of the fuel in consideration and the equivalence ratio (ratio of air to fuel). The effects of coal additives were not considered because an ultimate analysis of the coal was not available at the time. This information is now available, and it will be included in the program in the near future. Figure 18 shows the results obtained from this computer program. For the idealized experiment studied with the computer, Figure 18 shows that as the equivalence ratio decreases (excess air increases), the adiabatic flame temperature decreases. Figure 18 also shows that the adiabatic flame temperature drops as the amount of water in the emulsion increases for various levels of equivalence ratio. This analytical result compares favorably with the observed experimental relation between the amount of water in oil-water-air emulsions and the heat flux to a simulated load[20].

During the next quarter additional experiments will introduce increased percentages of coal in the oil-water-air emulsion. Upon completion of the construction of the probes, measurements of the flame emissivity will be performed. In addition, the computer program will be used to calculate the adiabatic flame temperatures for different percentages of coal in the oil-water-air emulsion.

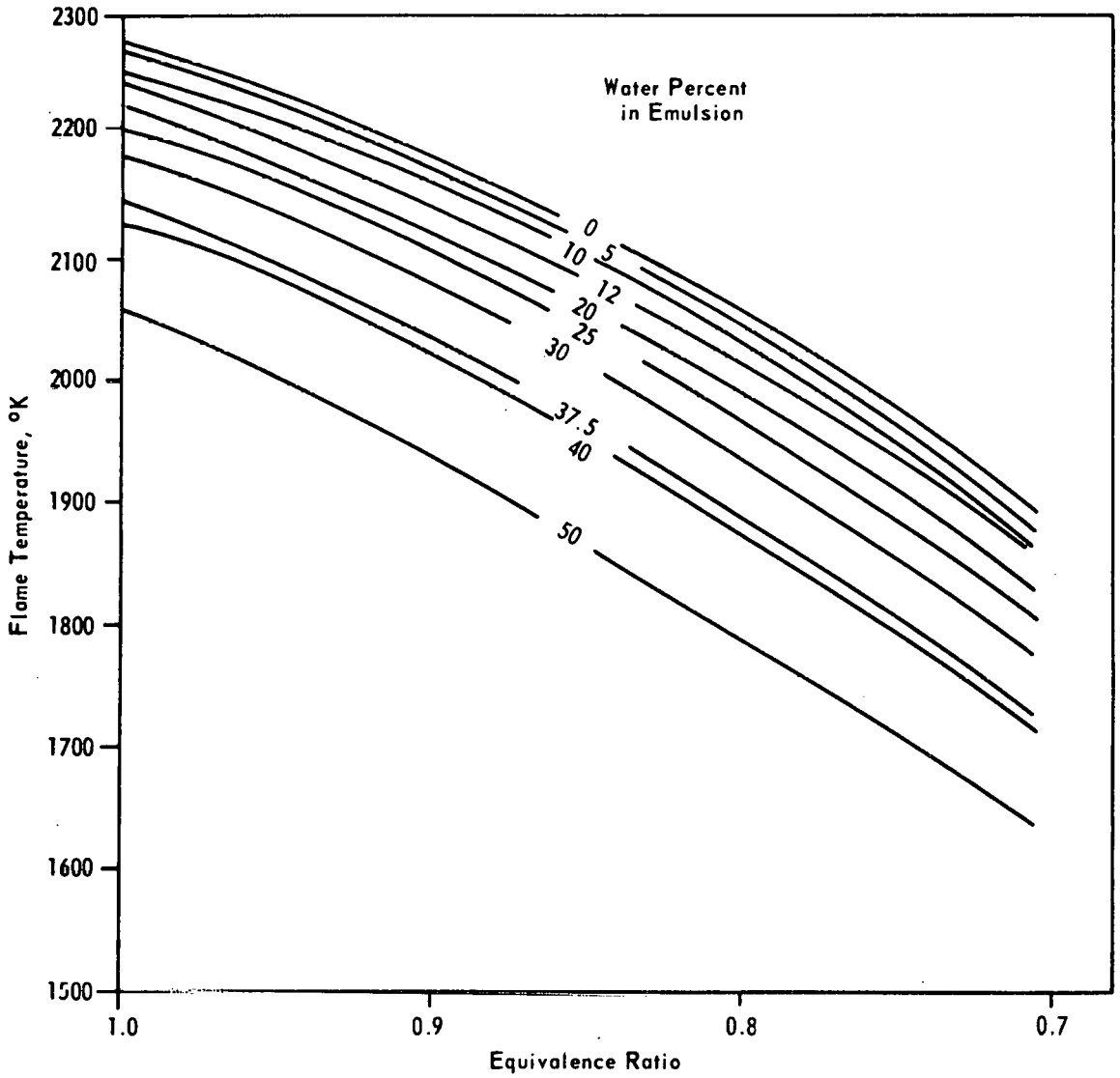

Figure 18. VARIATION OF ADIABATIC FLAME TEMPERATURE AS A FUNCTION OF EQUIVALENCE RATIO FOR DIFFERENT WATER-OIL EMULSIONS

CONCLUSIONS

1. Rapid Scan data output, or reflectograms, have been studied in an effort to determine the relative percentages of maceral constituents. Two methods of fitting maceral distribution curves (Gaussian) have been applied.

2. The combustion zone of a fuel bed of a laminar flow reactor is evidently diffusionally controlled, in agreement with past theories; but the gasification zone is not, in disagreement with past theories.

3. The calculations of coal particle temperature profiles under pyrolysis conditions indicate that in many cases the pyrolysis reaction can act as a "heat sink" and introduce substantial temperature gradients within the particle. Under these conditions the main pyrolysis zone within the particle is undergoing reaction at a temperature different from the external temperature.

4. Pyrolysis of pulverized coal in the laminar flow furnace occurs under essentially isothermal conditions.

5. Methanol densities of 13 char samples have been found to be very close to the helium densities. For a given sample, the difference between the two densities is less than 5 percent. Methanol densities show a drift with time, but in about 72 hr attain values which are comparable to the helium densities.

6. Small angle x-ray scattering studies show that the internal pore structure of coal chars changes with rank of the starting coal precursor and the maximum temperature at which the char is prepared.

7. Carbon deposition from the cracking of methane into the pores of a lignite char occurs at a significant rate at temperatures between 815 and 855°C. The maximum amount of carbon deposited is much less than the amount of open pore volume which is potentially available to accommodate carbon within the char. Removal of the inorganic impurities from the char by acid washing significantly reduces the extent of carbon deposition.

8. Removal of mineral matter from coals and chars markedly affects reactivity and surface areas of chars. The decrease in char reactivity and changes in surface area are less pronounced when the raw chars rather than the coal precursors are acid washed. Hydrogen addition to steam has an inhibiting effect on reactivity in most cases. Reactivity of a lignite char is independent of particle size in the range 40 x 100 to 200 x 325 mesh. However, reactivity of a LV bituminous char increases upon particle size reduction.

9. Ion exchange increases char reactivity to steam. There is a complex relationship between pore structure, catalyst behavior, and reactivity. Above 12.5 percent burn-off the order of activity of the catalysts is $Na > Ca > Fe = Mg$. No effect of end point pH of exchange on reactivity could be determined. K^+ containing char is more reactive than any of

the other exchanged chars. The nitrate and acetate anion have the same effect on charring and subsequent reactivity. Reactivity of thermally stable char is greater than predicted from reactivity of chars prepared from various exchanged coals.

10. Reactivity variation can be responsible for major shifts in combustor temperature profiles, according to a computer study of an infinite parallel plane combustor model. The fact that the plane-flame furnace used in the experimental facet of this project is of a fixed finite length does seem to magnify the differences between low and high reactivity fuels.

11. The addition of coal in water-oil emulsions has increased the heat absorbed by the water load on the furnace to levels comparable to that of fuel oil no. 2. Water additions in fuel oil no. 2 and higher levels of excess air reduce the adiabatic flame temperature.

REFERENCES

1. Walker, Jr., P.L., F. Rusinko, and L.G. Austin. Gas Reactions of Carbon, in Advances in Catalysis, Academic Press, N.Y., v. 11, p. 133, 1959.

2. Spackman, W., A. Davis, P.L. Walker, H.L. Lovell, R.H. Essenhigh, F.J. Vastola, and P.H. Given. The Characteristics of American Coals in Relation to Their Conversion into Clean Energy Fuels. Qtr. Tech. Prog. Rept. FE-2030-3 of The Pennsylvania State University to ERDA, 185 pp., May, 1976.

3. Juntgen, H., and K.H. van Heek. Gas Release from Coal as a Function of Heating Rate. Fuel, v. 47, p. 103, 1968.

4. Sparrow, E.M., and R.D. Cess. Radiation Heat Transfer (revised ed.). Brooks/Cole Publishing Company, p. 313, 1970.

5. Anthony, D.B., J.B. Howard, H.C. Hottel, and H.P. Meissner. Rapid Devolatilization and Hydrogasification of Bituminous Coal. Fuel, v. 55, p. 121, 1976.

6. Bartholomew, C.H., and M. Boudart. Preparation of a Well Dispersed Platinum-Iron Alloy on Carbon. J. Catalysis, v. 25, p. 173, 1972.

7. Dacey, J.R., and D.G. Thomas. Adsorption on Saran Charcoal. Trans. Faraday Soc., v. 50, p. 740, 1954.

8. Barton, S.S., J.B. Evans, and B.H. Harrison. An Investigation of the Pore Structure and Molecular Sieve Properties of Polyvinylidene Chloride Carbons. J. Colloid Interface Sci., v. 49, p. 462, 1974.

9. Ehrburger, P., O.P. Mahajan, and P.L. Walker, Jr. Carbon as a Support for Catalysis. I. Effect of Surface Heterogeneity of Carbon on Dispersion of Platinum. J. Catalysis, v. 43, p. 61, 1976.

10. Benson, J.E., and M. Boudart. Hydrogen-Oxygen Titration Method for the Measurement of Supported Platinum Surface Areas. J. Catalysis, v. 4, p. 704, 1965.

11. Gan, H., S.P. Nandi, and P.L. Walker, Jr. Porosity in American Coals. Res. and Dev. Rept. No. 61, I.R. No. 4 of The Pennsylvania State University to OCR, 15 pp., September 15, 1972.

12. Jenkins, R.G., and P.L. Walker, Jr. SAXS Studies on Carbons Derived from Polyfurfuryl Alcohol and Polyfurfuryl Alcohol-Ferrocene Copolymers. Carbon, v. 14, p. 7, 1976.

13. Walker, Jr., P.L., M. Shelef, and R.A. Anderson. Catalysis of Carbon Gasification, in Chemistry and Physics of Carbon, Marcel Dekker, N.Y., v. 4, p. 287, 1965.

14. Palmer, H.B., and C.F. Cullis. The Formation of Carbon from Gases, in Chemistry and Physics of Carbon, Marcel Dekker, N.Y., v. 1, p. 265, 1965.

15. Bokros, J.C. Deposition, Structure and Properties of Pyrolytic Carbon, in Chemistry and Physics of Carbon, Marcel Dekker, N.Y., v. 5, p. 1, 1969.

16. Hoffman, W. Unpublished results. The Pennsylvania State University, 1976.

17. Field, M.A. Rate of Combustion of Size-graded Fractions of Char from a Low-rank Coal Between 1200°K and 2000°K. Combustion and Flame, v. 13, p. 273, 1969.

18. Essenhigh, R.H., and J.G. Cogoli. Pulverized Char Combustion in a Laboratory Scale Furnace. 170th National Meeting ACS, Division of Fuel Chemistry, v. 20, no. 3, p. 134, 1975.

19. Gordon, S., and B. McBride. Computer Program for Calculation of Complex Chemical Equilibrium Compositions, Rocket Preformance, Incident and Reflected Shocks, and Chapman-Jouguet Detonation. NASA-SP-273, 1976.

20. Koval, A., S. Slupek, A. Kokkinos, A. Shaler, N. Mizkovsky, and R.H. Essenhigh. Smoke Point and Heat Transfer Characteristics of Oil/Water/Air Emulsions Without and with Coal Addition in a Hot Wall Furnace. Combustion Institute, Central States Mtg., Columbus, Ohio, April 1976.

The following individuals have made contributions to this report: C.P. Dolsen, T. Eapen, J. Friehaut, E.J. Hippo, D.S. Hoover, J.M. Hower, R.G. Jenkins, M. Kamishita, A. Kokkinos, K.W. Kuehn, A.A. Leff, A. Linares, O.P. Mahajan, N.Y. Nsakala, H.E. Shull, R.L. Taylor, and A. Youssef.

APPENDIX A

KINETICS OF GASIFICATION IN A COMBUSTION POT: A COMPARISON OF THEORY AND EXPERIMENT

by

Thomas Eapen
Graduate Assistant in Fuel Science
The Pennsylvania State University

Russell Blackadar
Technical Assistant in Fuel Science
The Pennsylvania State University

Robert H. Essenhigh
Professor of Fuel Science
The Pennsylvania State University

for

The 16th International Combustion Symposium
Cambridge, Massachusetts

SUMMARY

Reaction of carbon with air in a fixed fuel bed is shown to be controlled by diffusion in the combustion region of the bed, in agreement with all past theories and assumptions, but it is chemically controlled in the gasification region, contrary to most previous assumptions, with a temperature coefficient equivalent to 50 kcal. activation energy. The combustion pot in which the experiments were carried out was refractory lined (with 2.5" walls), of rectangular cross-section (6.5" x 15.5"), and with a bed up to 18" deep resting on a perforated steel plate as a grate. Fuel was mostly coke, in three size grades (approx. 1", 0.625", and 0.375"), with one size grade of coal. Gas compositions of O_2, CO_2, and CO were measured down through the bed. Experiments were carried out at 5 different air rates (5, 10, 15, 20, and 40 scfm): both air and gasification rates overlap with rates found in commercial gasifiers. The results were also compared with Kreisinger's data. The theory used an approximate solution to a prior analysis by Kuwata et al (3) for comparison with the experimental results. Kinetic coefficients were obtained from slopes of log/linear plots of gas compositions with time, notably of $(O_2 + CO_2)$. The velocity constant for the oxygen reaction in particular was found to be proportional to the 0.7 power of the velocity, in agreement with theory. The constant for the CO_2 reaction, however, was found to be highly temperature dependent, with a slope on an Arrhenius plot equivalent to 50 kcal. This generates gasification rates substantially lower than would be possible if the gasification reaction were diffusionally controlled. The results can provide a basis for the mathematical modelling of shaft reactors such as the Morgan or the Wellman-Galusha, with possible extension to the Lurgi which is pressurised and with oxygen and steam in place of air. The results may also be relevant to the problem of underground gasification.

1. INTRODUCTION

Although the diffusion theory of reaction control in a porous fuel bed has been most generally used in the last few decades for describing behavior in such systems as shaft gasifiers or underground gasification, evidence in support has never been entirely convincing. In 1963, Sherman and Landry (1) concluded in a major review that: "No completely satisfying theory of gasification in a fuel bed yet exists"; and as recently as 1975, Stewart and Kirov (2) concurred. This lacuna provided the incentive for the direction of this present work. We present here extension of a theory (3) that allows for non-diffusional control assumptions in the kinetic behavior, together with experimental support for the major elements of the analysis by measurements in a combustion pot.

2. EXPERIMENTAL

2.1 Combustion Pot - This is illustrated in Fig. 1. In essence, it is a refractory box, of rectangular cross-section, with a grate at the bottom, standing above a plenum chamber for the air supply. The refractory is 2½" series, FR 28 hot face insulation brick cased in 1/8" mild steel sheet, to give inside dimensions: 11½" by 20½"; and outside 16½" by 25½". The pot is bricked up to a height of 19½" allowing possible bed depths of 18". The grate is a 3/8" steel plate drilled with 112 holes (1/2" dia) set in a 7 by 16 matrix. The rectangular air plenum is also 11½" by 20½", by 6" deep, surmounting a conical ash hopper (also 6" deep) from which it is separated by an aluminum grating. The ash hopper can be cleaned through a 4" pipe-threaded plug. Air is supplied to the plenum through two 2½" dia baffled apertures located as shown in Fig. 1. The baffles are square

mesh aluminum grating bent to an optimum shape to ensure uniform air flow into the bed above. This was determined experimentally using a low velocity hot wire anemometer.

The pot is surmounted by a conical, refractory-lined hood pierced with two angled observation ports, and with provision, as indicated, for insertion of water-cooled probes for temperature and gas sample traverses vertically down through the bed. The off-gases are led up through the concial hood, through a tunnel with an afterburner, to the exhaust stack. A damper is provided in the tunnel section to allow operation at balanced draft.

Pressure taps are fitted to the air plenum below the grate and to the hood above the grate. Temperature profiles up the inside wall surface are measured by Pt-Pt/10%Rh thermocouples in mullite wells through the walls. Some indication of locations is given in Fig. 1.

The bricks were set in dry, to aid replacement when necessary, but they were sealed with two coats of France V-44 surface seal. The pot and ash hopper were mounted on wheels so that the bottom part of the unit could be easily detached from the hood above, both for assisting light-off and for certain experiments. Opposing edges of both hood and pot were fitted with steel angle that could be bolted together, with an asbestos-graphite fiber gasket between to prevent leakage. (To permit the movement, air was supplied to the plenum through flexible hoses).

2.2 Probes and Related Ancillaries - Temperatures in the bed were measured with a sheathed thermocouple, 6" long, held at the end of a 3/8" dia tubular steel shaft, 48" long. This was inserted into the bed as shown in Fig. 1 and elevated up and down as required.

For the gas sampling, two different probes were used. Both were water-cooled, 60" long. The first was 3/4"o.d., and the second was 5/8" o.d. The two different sizes were used to check the effect of the probe itself in the bed. The smaller diameter probe was found to be much easier to push into the bed, and it evidently reduced channeling and local cooling. As a further check on this, some few runs were made with a 1" dia mullite tube covering the end 15" of the probe. This further reduced local cooling, but the coverings were easily broken by mechanical and thermal shock before a complete pass through the bed could be made.

A diaphragm pump was used to draw out the gas samples. Samples passed successively through two wash bottles, a drying tower and filter, the pump, a rotameter, secondary drying, particulate traps, and then to the gas analysers.

2.3 Instrumentation - Air supplied from a 20 oz blower was metered by rotameter (range 0 to 45 cfm). Pressure differentials in the bed from the pressure taps were measured by Bristol inverted-bell draft gage reading from +0.05" w.c. to -0.15" w.c. Wall temperatures were recorded by a Speedomax (L & N) potentiometric 24-point recorder. This was also used when traversing the bed with the inserted thermocouple.

Bed and off-gases were only analysed for O_2, CO_2 and CO, using separate on-line analysers. Carbon monoxide and dioxide were determined by separate MSA Model 300 LIRA's, both calibrated for zero to 25%. Oxygen was obtained by a L & N Thermomagnetic analyser, with a Speedomax H readout (zero to 20% calibration). Calibrations were periodically checked using appropriate calibration gases.

2.4 Fuel Preparation - Foundry-grade coke was used in these experiments in sized pieces of approximately 4" mean diameter. These pieces were then crushed, mostly by hammering (use of the mechanical crusher resulted in too many fines), in lots of about 100 lb. The pieces were then sized by hand using standard twelve-inch square-mesh sieves with opening sizes 0.25", 0.5", 0.75", and 1.25" to give nominal particle sizes 0.375" (±0.125"), 0.625" (±0.125"), and 1.0" (±0.25"). About 25 lb of the sized coke was used for each experimental run.

For one run, a nonswelling subbituminous B coal was used (PSOC designation 322, volatile matter 32.53% d.m.m.f.). This was prepared in the same manner as the coke to a nominal size of 0.375" (±0.125").

2.5 Light-off and Procedure - To light-off, 2 to 5 lb of cookout charcoal soaked in starting fluid was placed in the pot and lit, with the pot rolled away from under the off-gas hood. This charge was allowed to burn for 10 minutes at an air rate of 5 scfm. The coke charge was then added, to the desired depth, generally 15", and the pot was rolled under the hood and sealed to it. The air rate was then set at the desired level, and left for 20 to 80 minutes to reach steady state (the time depending on the air rate). The probe was then pushed into the bed and the system left to stabilize for taking the first gas analyses (usually taking about 3 minutes). If the probe clogged during the sampling, which occurred quite frequently, the clogging particles were removed by back-flushing with compressed air. After each station reading, the probe was inserted further into the bed and new measurements were taken.

When samples had been taken all the way down to the grate, the probe was removed and the process repeated. Before re-inserting the probe, however, the bed was allowed to readjust and fill up the hole in the bed left by the probe. (The creation of this hole meant that samples taken at successive stations by withdrawing the sampling probe were suspect). On re-inserting, the probe was first used to measure the bed height by moving it down to contact the top of the bed (checked visually) and noting the position on a vertical scale on the probe mount. These measurements were used to check the burn-off. When the bed was very low or had burned out, taking 100 to 300 minutes, the run was terminated. After the pot had cooled, it was opened, and all ash, clinker, unburned coke and ash pit contents were removed and weighed.

Typical profiles obtained are illustrated in Fig. 2.

3. THEORETICAL

3.1 Rate Equations (Summary) - For simultaneous reaction of oxygen and CO_2 with carbon and homogeneous gas-phase reaction of CO with oxygen in the bed interstices, the rate equations for disappearance of oxygen (dN_1/dt) and CO_2 (dN_2/dt), as obtained by Kuwata et al (3), are

$$dN_1/dt = -n_1 N_1 - (1/2) n_3 N_3 [N_1/(1 + N_3/2)]^m \quad (1)$$

$$dN_2/dt = -n_2 N_2 + n_3 N_3 [N_1/(1 + N_3/2)]^m \quad (2)$$

where N_i is the local mole fraction of the reactive gases (i = 1, 2, or 3 for O_2, CO_2 or CO, respectively) per entering mole (oxygen plus nitrogen);

n_i are reaction velocity constants for the O_2 and CO_2 reactions, per unit interstitial volume (ϵ) in the bed, given by $n_i = (A_s/\epsilon)k_i$ where A_s is the available solid surface for reaction per cubic foot of bed, and k_i are the true (first order) velocity constants for reaction of O_2 and CO_2 with carbon. The gas phase reaction (CO/O_2) was treated phenomenologically (3), because of the complexity of the mechanism, with reaction first order in CO and fractional-order (m) in O_2 as discussed in the evaluation of this reaction by Johnson (4).

The true local mole fraction (Y_i) as measured by gas analysis in the bed is related to the mole fraction per entering mole (N_i) by

$$N_i = Y_i/(1 - Y_3/2) \quad \text{or} \quad Y_i = N_i/(1 + N_3/2) \tag{3}$$

and the local mole fraction balance can be written

$$Y_1^o = Y_1 + Y_2 + (Y_3/2)(1 + Y_1^o) = N_1 + N_2 + N_3/2 \tag{4}$$

Dividing Eq. 2 by two and adding Eq. 1 yields

$$(d/dt)(N_1 + N_2/2) = -n_1 N_1 - n_2 N_2/2 \tag{5}$$

3.2 Solutions - (i) For $n_i = n_2$ we obtain the diffusional solution assumed in virtually all previous analyses. Equation 5 integrates to yield (3)

$$(N_1 + N_2/2) = (Y_1 + Y_2/2)/(1 - Y_3/2) = Y_1^o \exp(-n_1 t) \tag{6}$$

noting that $Y_1^o = N_1^o$ = the entering oxygen mole fraction.

(ii) For $n_1 \neq n_2$, a solution exists, but the equations are too intractable to obtain the exact solution. An approximate solution that gives us sufficient basis for experimental evaluation can be obtained by first writing Eq. 5 in the form

$$(d/dt)(N_1 + N_2/2) + n_2(N_1 + N_2/2) = (n_2 - n_1)N_1 \qquad (7)$$

Clearly, this can be solved if we know N_1 as a function of time. From Fig. 2 we note that the CO concentration (N_3) is low or zero over much of the oxygen decay so that Eq. 1 would yield: $N_1 \simeq N_1^o \exp(-n_1 t)$. Also from Fig. 2 we note that when N_3 becomes significant, N_1 is small or zero and Eq. 7 can be solved directly. Hence, writing $N_3 = \sum_1^\infty a_j t^j$ enables us to substitute in Eq. 1 and solve for N_1 knowing that the solution must approximate to the exponential decay at low t and go to zero as N_3 becomes significant. Substituting in Eq. 7 for N_1 thus obtained, and integrating, yields

$$(N_1 + N_2/2) = Y_1^o [A(t).\exp(-f(t).t) + (1-A_o)\exp(-n_2 t)] \qquad (8)$$

where $f(t) = n_1 + n_3 \sum_1^\infty [a_j/(1+j)]t^j$; A(t) is a double summation of the modified series for N_3; and A_o (a constant) is the value of A(t) at t = o. Alternatively, we note that the oxygen decay can be approximately modelled by an arbitrary exponential decay that may be written: $N_1 \simeq N_1^o \exp(-nt)$; whence an alternative approximate solution to Eq. 7 is obtained of the form:

$$(N_1 + N_2/2) \simeq A\exp(-nt) + B\exp(-n_2 t) \qquad (9)$$

where $A = Y_1^o (n_1 - n_2)/(n - n_2)$; and $B = Y_1^o (n - n_1)/(n - n_2)$. We can also

say that $n \simeq n_1$ at low t so that we can obtain expressions for n or n_1 as functions of velocity, temperature, and so forth. Note, that if we take exactly: $n = n_1$; $A = N_1^o$, and $B = 0$. The difference between Eqs. 8 and 9 appear only in the first R.H.S. term.

4. RESULTS AND ANALYSIS

4.1 General Behavior - The general behavior of the gas concentration profiles inside the bed is as illustrated in Fig. 2. These profiles, showing the variability of measurements taken 60 minutes apart, are quite typical of what has been reported by others in the past.

Temperatures in the bed varied with porosity (particle size), and velocity, as expected. Temperature across a horizontal plane was surprisingly uniform, but varied from bottom to top, rising from cold ambient at entry, to a peak within an inch or two, and declining slowly thereafter. The average bed temperatures ranged from 950°C to 1550°C.

Gasification rates ranged from 5 to 25 lb/sq.ft.hr., which overlaps the range in full scale gasifiers (10 to 50 lb/sq.ft.hr.). The Reynolds Numbers in the bed pores were estimated (by estimating pore diameters) at 200. With comparable gasification rates and particle sizes to those used in full scale, the Reynolds Numbers here should therefore translate to the full scale.

The variation of particle density, to indicate the presence or absence of internal particle reaction, was also investigated. The reaction was stopped part way through a run by removing the pot from under the exhaust hood and covering it with a steel plate until cold. The bed was then removed in horizontal slices which were weighed, and the particle volumes in the slices measured to determine density. Particle density from top to

bottom was found to be reasonably constant. Particle size, just as clearly, diminished from top to bottom. Bed porosity also changed. It can be taken therefore that reaction was mostly at the superficial particle surface, and not internal. This finding is consistent with diffusion reaction control or Zone II reaction with minimal penetration.

4.2 Evaluation of Probable Mechanisms - Potential for differentiating between possible mechanisms is provided by the alternative solutions to Eq. 5, namely Eqs. 6 and 8 or 9. For (approximately) equal kinetic constants in the heterogeneous reactions ($n_1 = n_2$), a log/linear plot of $[(O_2\% + CO_2\%/2)/(1 - CO\%/2)]$ against time should yield a straight line. For $n_1 \neq n_2$, a curve should be generated.

Figure 3 is typical of the results obtained for two of the particle sizes examined. Similar plots were obtained for other particle sizes, including coal and Kreisingers coke data (5). Clearly, the qualitative trend obeys Eq. 8 or 9, not 6.

The kinetic constants, n and n_2, are given by tangents to the curves at $t = o$ and $t = \infty$, respectively. Evidently, $n_2 < n(=n_1$ at $t = o)$. The gasification reaction (n_2) must therefore be kinetically, not diffusionally determined. Choice of mechanism for the combustion region is less clear cut. On the basis of the evidence of Fig. 3, however, a kinetic interpretation is improbable since the bed temperature in the combustion region is changing rather rapidly. Since the kinetically controlled O_2/C reaction is known to have a very high temperature coefficient (governed by an activation energy in the range 20 to 40 kcal), this would show up as a concave downward slope on Fig. 3 of increasing steepness in the initial

region. The slopes for n and n_2 would also be similar, differing by a factor of 2 or less instead of the factor of up to 10 observed. With a diffusion mechanism, the temperature coefficient is quite small. Identification of the combustion region as diffusionally controlled is therefore somewhat better supported. It is also in line with past attempts to model such systems (e.g. 6 - 13) which were always reasonably successful in the combustion zone (but predicting rates in the gasification zone that were almost invariably much too high).

4.3 Gasification Velocity Constant - Limiting slopes (n_2) of the Fig. 3 and allied curves were evaluated at large time by two methods: first, by drawing tangents to the curves; and second, by obtaining best fit values that would match the original gas composition profiles (Fig. 1).

Figure 4 illustrates an Arrhenius plot of the results (n_2 against 1/T) for the three coke sizes and one coal, with Kreisingers data of 1916 for comparison. The slopes, including Kreisingers data, are approximately parallel, and correspond to an activation energy of about 50 kcal., thus establishing beyond doubt that the gasification reaction is not diffusion controlled.

4.4 Combustion Velocity Constant - To evaluate n ($\simeq n_1$), the expression given by Spiers (14) for the transfer coefficeint ($k_1 = n_1\ \varepsilon/A_s$) for a particulate bed was used:

$$St = k_1/V = 4.32[(1 - \varepsilon)/d](Vd/\nu)^{-0.3} \qquad (10)$$

where St is the Stanton Number, V is the gas velocity relative to the empty container, d is the particle size, and ν is the kinematic gas viscosity.

Both porosity, ε, and surface area, A_s, are functions of diameter. Using: $A_s = 6(1 - \varepsilon)/d$; for spherical particles, and evaluating the group $(1 - \varepsilon)^2/\varepsilon$ as proportional to d^m with m between 1.5 and 2, rearrangement of Eq. 10 yields

$$n \simeq n_1 = K V^{0.7} \tag{11}$$

$$\text{where } K = K_o d^{-0.3 \text{ to } -0.8} \tag{12}$$

and K_o is a constant.

To test these equations, Fig. 5 is a log/log plot of n against velocity where the solid lines are least squares fit to the experimental points and the dashed lines are the 0.7 slopes. The good agreement is evident. The equation constant, K, was then determined from separate plots of n against $V^{0.7}$, and the values obtained plotted against diameter, d, on a log/log plot. Best least squares fits were found to yield an index of -0.7 which is bracketed by the estimate of -0.3 to -0.8 indicated by Eq. 12. Figure 6 is a plot of K against $d^{-0.7}$ to illustrate the equation and to show the effect of the different fuels on the parameter K_o.

These results reasonably establish agreement on the functional form of the equation relating n to V and d. Evaluation of the final constant K_o, for closure in the calculations, was somewhat less successful but this can be attributed to accumulation of the errors of assumption and approximation. The "theoretical" value of K_o was in the region of unity whereas the experimental values (slopes of lines of Fig. 6) were 0.4 for the coal, 0.26 for the coke, and 0.9 for Kreisinger's coke data.

5. DISCUSSION AND CONCLUSIONS

Our findings are: that the combustion zone of a fuel bed is evidently diffusionally controlled, in agreement with past theories and conclusions; but the gasification zone is not, in disagreement with past theories. This last is considered to be the most significant finding, together with the estimate of the activation energy involved, of about 50 kcal. The practical significance of such a high temperature coefficient in a reactor is self evident. What may also be new is the direct experimental evaluation or validation of the velocity and diameter functions in the combustion zone.

The activation energy of the C/CO_2 reaction in non-diffusional systems has, of course, been measured before, with values found in the range 25 to 80 kcal., which brackets our value (15). Part of the variation is due to the difference between Zone I and Zone II measurements. Zone I behavior would, of course, show up as a drop in density which was not observed. Zone II behavior at constant density implies that reaction is confined to a thin surface zone that is too thin to be detected by gross density changes; it would also mean that the true activation energy is closer to 100 kcal., which is high but not impossible.

The results also focus attention on the need for better information on a number of parameters if acceptable predictions are to be obtained from mathematical models of shaft reactors and *in situ* gasification. Factors of particular concern are: the internal surface area of the bed; the variation of bed porosity with particle size; the extent of internal reaction that is probably occurring in the gasification zone; and the behavior of the CO kinetics in the bed.

SYMBOLS

A_s	solid surface area per unit volume
A	$Y_1^o(n_1 - n_2)/(n - n_2)$
B	$Y_1^o(n - n_1)/(n - n_2)$
d	particle diameter
K	velocity equation constant
k_i	true velocity constant
m	reaction order in Eqs. 3 and 4
N_i	local mole fraction per entering mole
N_1^o	entering oxygen mole fraction = Y_1^o
n_i	$k_i A_s/\varepsilon$
St	Stanton number
t	transit time
V	velocity in the empty chamber
x	distance above the grate
Y_i	true local mole fraction of the i^{th} component
Y_i^o	entering oxygen mole fraction = N_1^o
ε	porosity of the bed
ν	kinematic viscosity
η	dynamic viscosity
ρ	density

Subscripts

1	oxygen
2	carbon dioxide
3	carbon monoxide

Acknowledgements

This work was supported by the Pennsylvania Science and Engineering Foundation under Grant Number 231, and whose support is appreciatively acknowledged. We also wish to acknowledge crucial contributions from Mr. R.A. Frank, Research Aide, and Mr. Carl J. Martin, Machinist, who built the equipment. The work is continuing under ERDA Contract No. E(49-18)-2030.

REFERENCES

1. Sherman, R.A., and Landry, B.A., Chemistry of Coal Utilization: Supplementary Volume (H.H. Lowry: Ed.); Ch. 18; John Wiley, 1963.

2. Stewart, I.M., and Kirov, N.Y., 15th Symp. (Internat.) on Combustion, p. 1601. The Combustion Institute, Pittsburg, Pa. 1975.

3. Kuwata, M., Kuo, T.J., and Essenhigh, R.H., Proc. 4th ASME National Incinerator Conf., p. 272 (1970).

4. Johnson, M.L.M., and Essenhigh, R.H., A.I. Chem. E. Symp. Series No. 126, 68, 311 (1972).

5. Kreisinger, H., Ovitz, F.K., and Augustine, C.E., U.S. Bur. Min., Tech. Pap. No. 137, 1916.

6. Rosin, P.O., J. Inst. Fuel 11, 26 (1937).

7. Mayers, M.A., Chemical Rev. 14 31 (1934); Trans. Amer. Soc. Mech. Engrs. 59 279 (1937); Ind. Eng. Chem. 32, 563 (1940).

8. Bennet, J.G., and Brown, R.L., Gas J. 232 378 (1940).

9. Thring, M.W., Coal Research, Sept., p. 70 (1940); J. Inst. Fuel 19, 47 (1940); Fuel 31, 355 (1952).

10. Hougen, O.A., and Watson, K.M., "Chemical Process Principles", Wiley pp. 1068-74 (1947).

11. Silver, R.S., Fuel 32, 121 (1953).

12. Spalding, D.B., Proc. Inst. Mech. Engrs. 168, 545 (1954).

13. Silver, R.S., and Mackay, R.W., Brit. J. Appl. Phys. 6, 267 (1955).

14. Spiers, H.M., Technical Data on Fuel, 6th Ed., p. 80 Brit. Nat. Comm. World Power Conf. (1961).

15. Walker, P.L., Rusinko, F., and Austin, L.G., "Gas Reactions of Carbon", in Advances in Catalysis XI, 133-221 (1959).

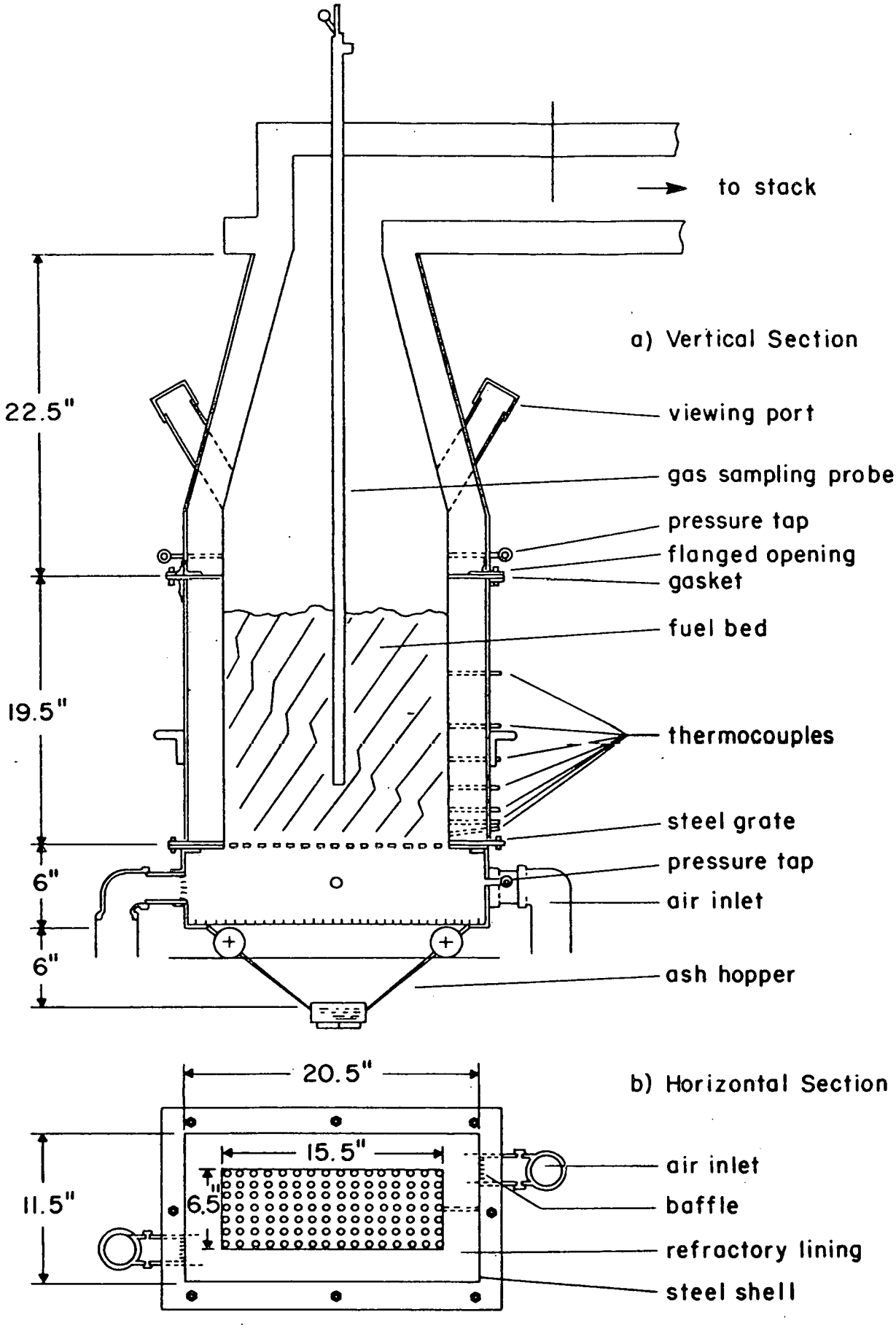

Figure 1 - Combustion Pot

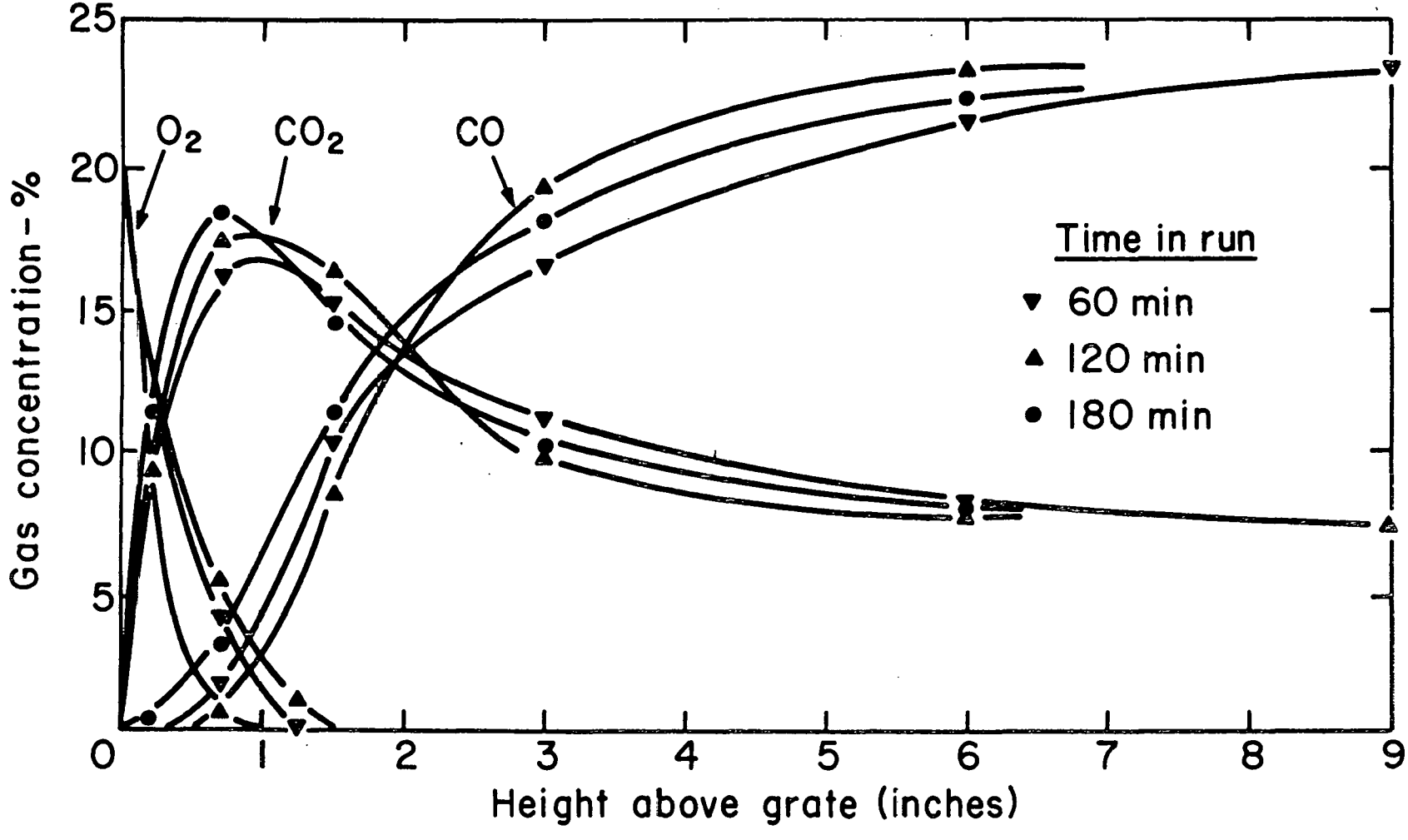

Figure 2 - Variation of Gas Compostion with Height Above Grate
[Coke 0.375"; air flow 5 scfm] at different times

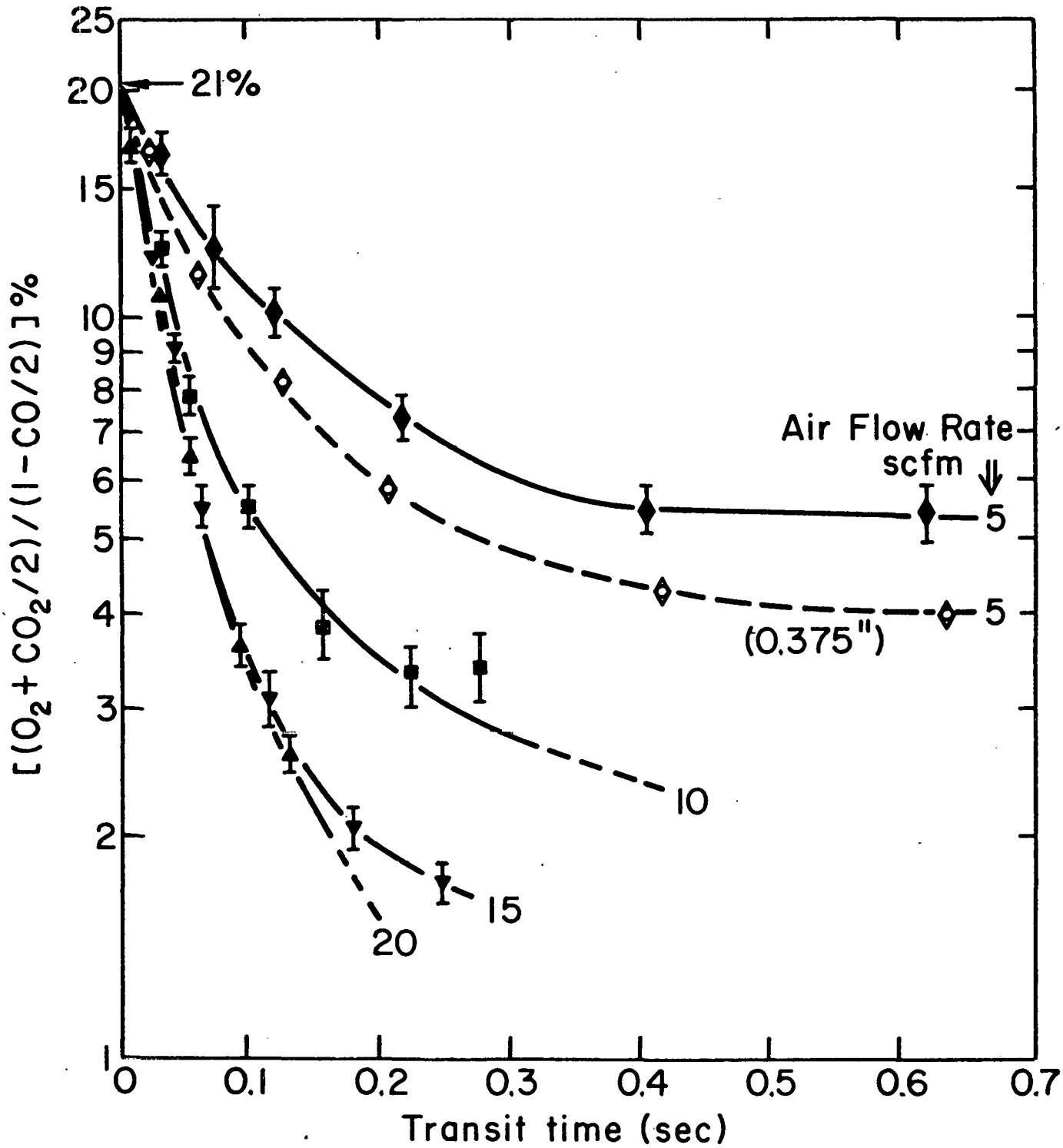

Figure 3 - Variation of $[(O_2 + CO_2/2)/(1 - CO/2)]$ with time [Eq. 9a] for 0.625" coke particles at 4 air flow rates, and for 0.375" coke particles at 5 scfm air flow rate (dashed line)

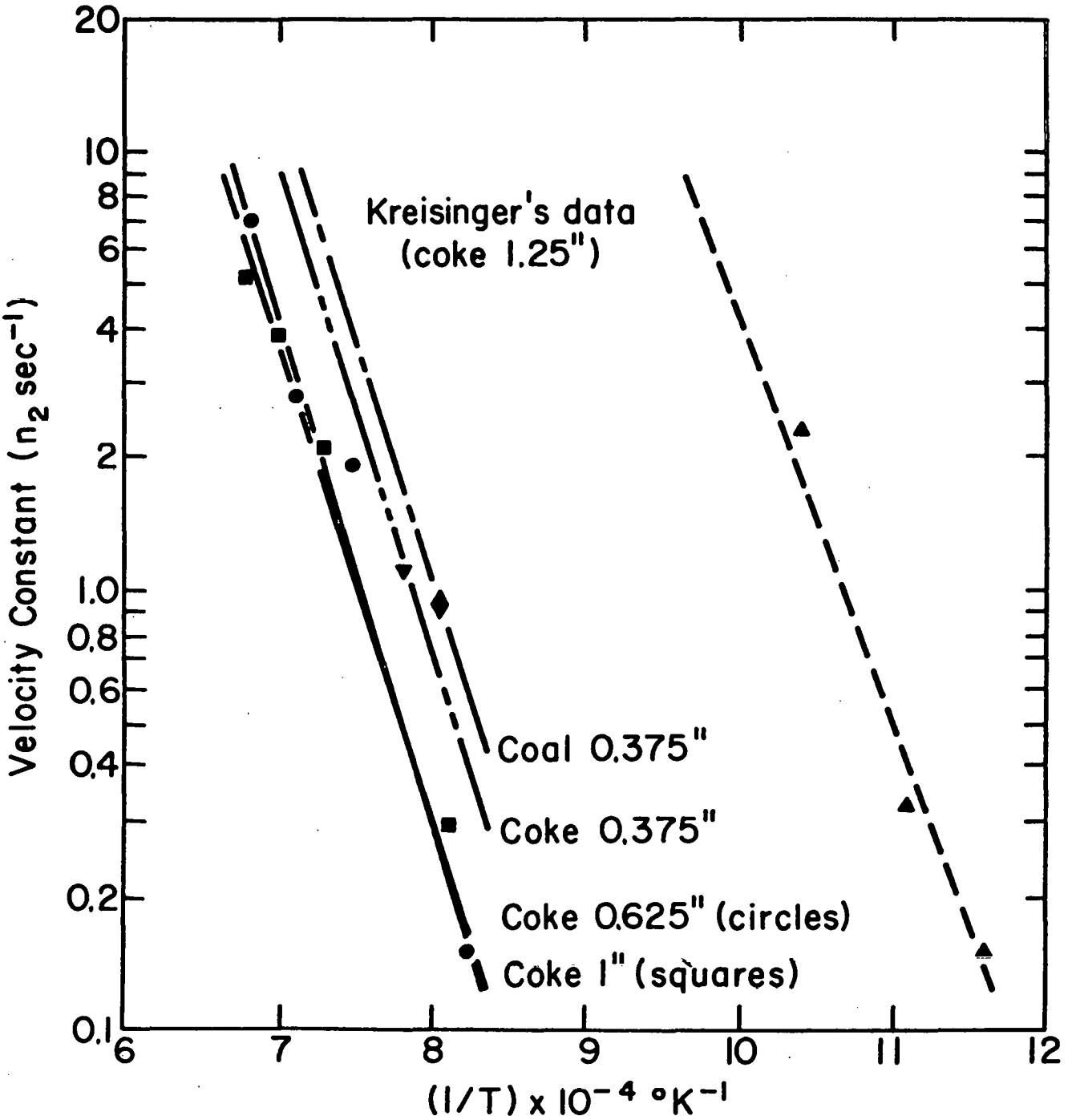

Figure 4 - Arrhenius Graph of Velocity Constant n_2 with Temperature

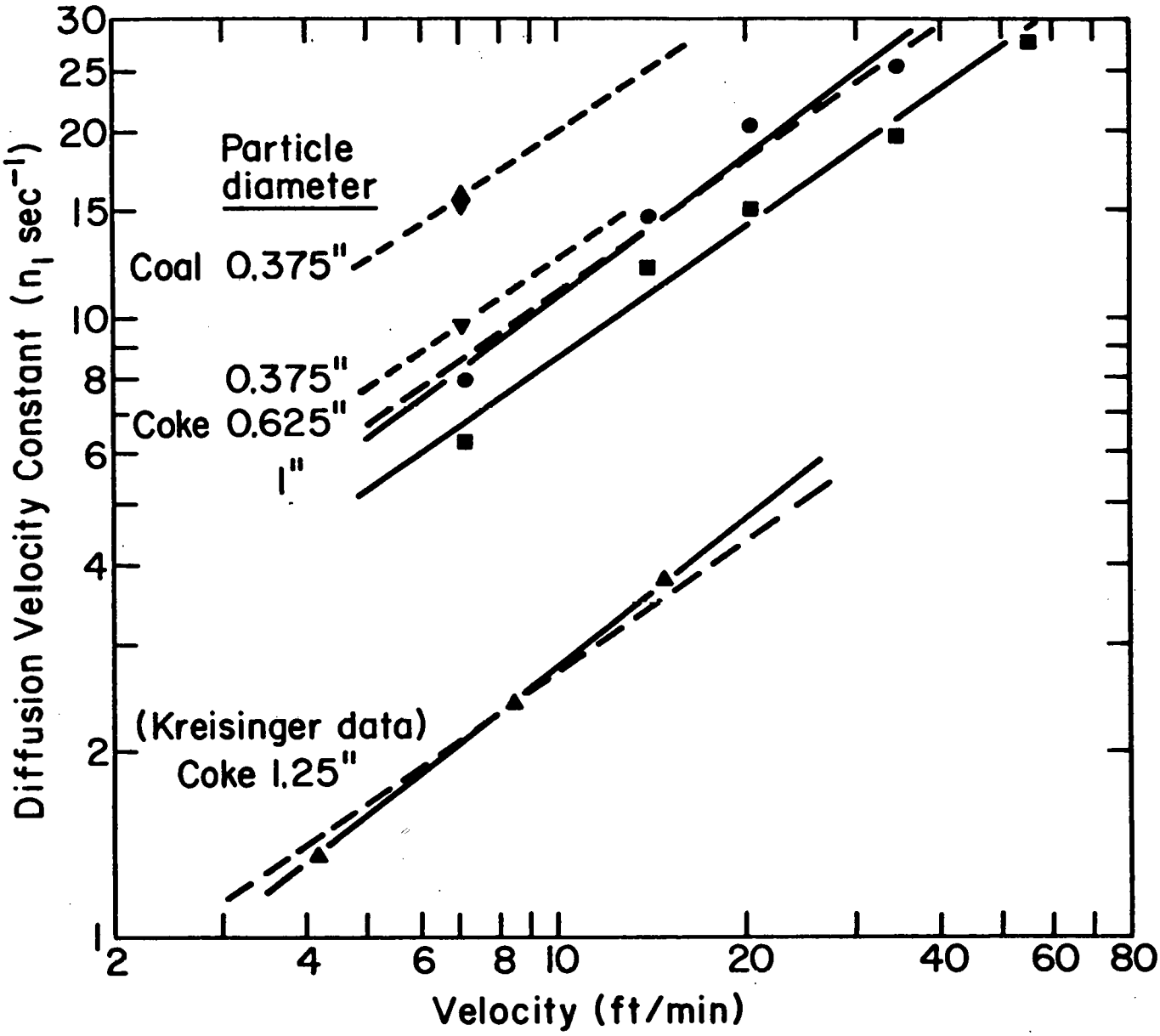

Figure 5 - Variation of Diffusion Velocity Constant n_1 with Velocity. Solid lines are least squares fit; dashed lines are slope 0.7 in accordance with Eq. (11). Data from Kreisinger (14) are also included (bottom line)

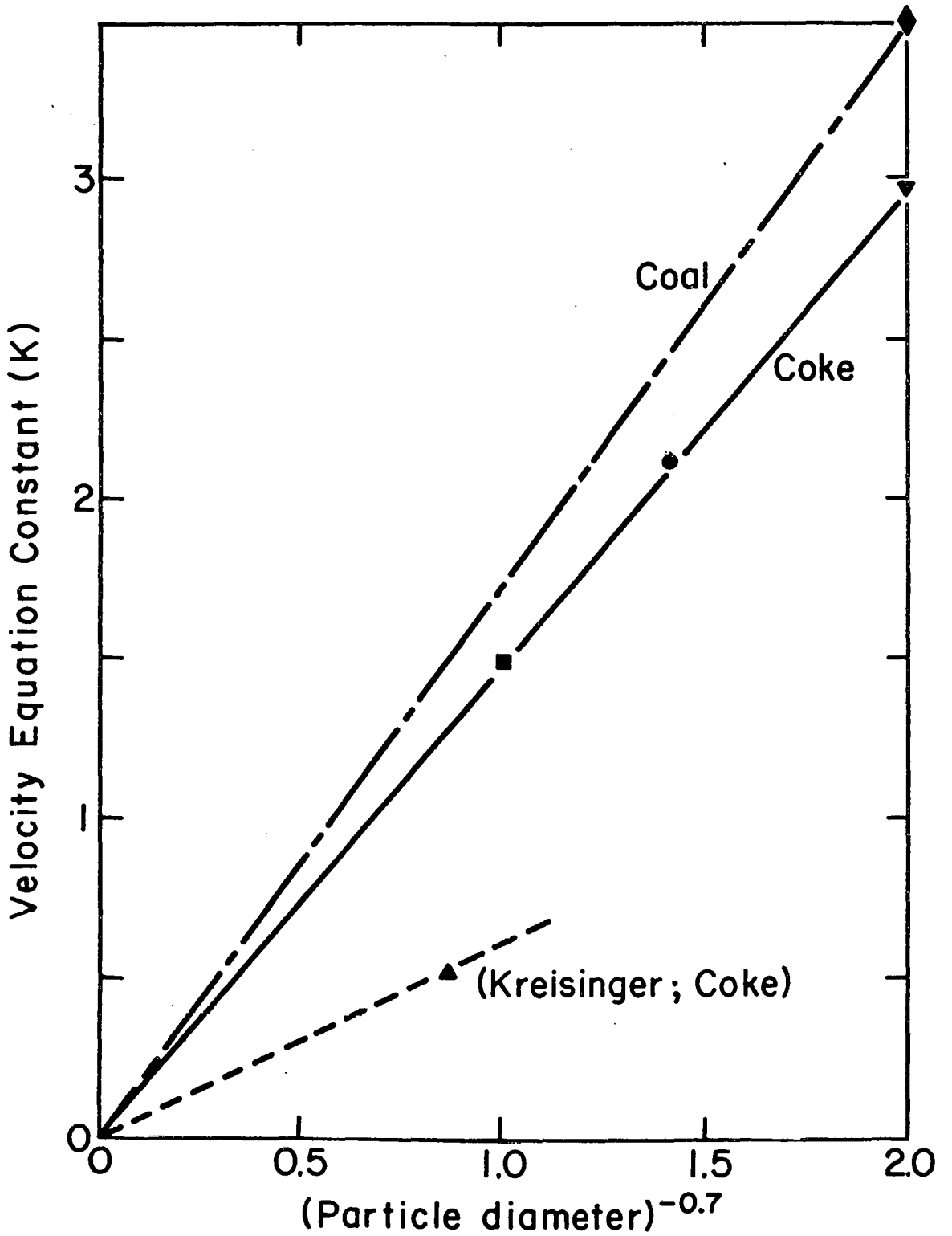

Figure 6 - Variation of Velocity Equation Constant (K) [Eq. 13] with (Particle diameter)$^{0.7}$

☆ U.S. GOVERNMENT PRINTING OFFICE: 1977 740 091/164